

CHEM 357/PHYSICAL CHEMISTRY LAB

EXPERIMENT PACKET

- 1. THE KINETICS OF A HOMOGENEOUS REACTION IN SOLUTION
(SOLUTION KINETICS)**
- 2. THE KINETICS OF A DIFFUSION-CONTROLLED REACTION
(FLUORESCENCE)**
- 3. VISCOSITY OF LIQUIDS PART I: LOW VISCOSITIES**
- 4. POLYMERS**
- 5. EMISSION SPECTROSCOPY: BIOPHYSICS AND FRET**
- 6. NMR DETERMINATION OF KETO-ENOL EQUILIBRIUM CONSTANTS**

Experiment 21

The Kinetics of a Homogeneous Reaction in Solution

Objective To measure the rate constant of the reaction between 2,4-dinitrochlorobenzene and piperidine in solution; to test the reaction mechanism; and to determine the Arrhenius parameters of the reaction.

Introduction From both a practical and a theoretical point of view, we can get valuable quantitative information about the rate of a chemical reaction, including the way in which the rate depends on the concentrations of all relevant chemical species and on the temperature. We can use this information, for example, to predict the rate of reaction under a given set of conditions (i.e., concentrations). We can also use this knowledge to adjust the conditions affecting the reaction so that it can be tailored to a specific application. Moreover, the information obtained concerning the dependence of the reaction rate on the conditions can provide us with an understanding of how, on a molecular level, the reaction actually takes place, i.e., the *mechanism* of the reaction.

First we will introduce some basic aspects of reaction kinetics. Consider a general chemical reaction in which the reactants *and* products are known. The balanced equation is written as



The speed of the reaction can be determined by measuring either the rate of disappearance of a reactant or appearance of a product. The actual magnitude of the reaction rate will depend on which species is being measured because of the stoichiometric relationship that exists between these species.

The rate of reaction, or reaction velocity, v , is simply

$$v = \frac{1}{v_i} \frac{d[X_i]}{dt}, \quad (2)$$

where $[X_i]$ is the molar concentration of the i th species, and v_i is the stoichiometric coefficient of the balanced equation. The rate, v , is always positive because for a reactant, both v_i and $(d[X_i]/dt)$ are negative (the reactant concentration decreases with time); for a product, both v_i and $d[X_i]/dt$ are positive quantities.

In general the reaction rate, v , is a function of the concentration of one or more of the reactants and, sometimes, products. In addition, v is almost always found to depend on the temperature, T , and sometimes on the reaction medium, e.g., the solvent. Thus,

$$v = f([X_1], [X_2], [X_3], \dots [X_N], T) \quad (3)$$

The equation represented in (3) is called a *differential rate law*. Note that, in general, the concentration terms, $[X_i]$, in equation (3) are time-dependent, and thus v is also time-dependent.

As the reaction proceeds, the rate almost always decreases. With respect to the general reaction illustrated in equation (1), we can express the rate law as

$$v = k[A]^{\alpha}[B]^{\beta}[C]^{\gamma}[D]^{\delta}[Y]^{\epsilon}, \quad (4)$$

where k is a constant (independent of time) called the *rate constant*, $[A]$, $[B]$, ... are the molar concentrations, and $[Y]$ is the concentration of a species not represented in the balanced equation but that nevertheless affects the rate of reaction. The point to be made about the expression in (6) is that the chemical species all appear as factors in the rate law, and they are all raised (in general) to different exponents. The exponent to which a particular species concentration is raised is called the *order* of the reaction with respect to that species. The *overall order* is the sum of exponents in a rate law such as (4).

We must strongly emphasize the following points: (a) We do not know in advance of actually determining the rate law [equations (3) or (4)] which chemical species actually appear in the expression, and (b) there is not necessarily any relationship between the stoichiometric coefficient of a species in the balanced equation (1) and the power to which that species (concentration) is raised in the rate law.

The rate law can be determined only by experiment, and it is the form of the rate law thus obtained that relates to the mechanism of the reaction. Conversely, the mechanism deduced for a reaction leads to a prediction of what the rate law for the reaction should be. That mechanism can thus be tested by comparing the predicted and experimentally determined rate laws.

Usually, the exponents in the rate law are integers (or sometimes, usually in gas phase systems, rational numbers — the ratio of two integers). For reactions in solution, these exponents are commonly 1, 2, or -1.

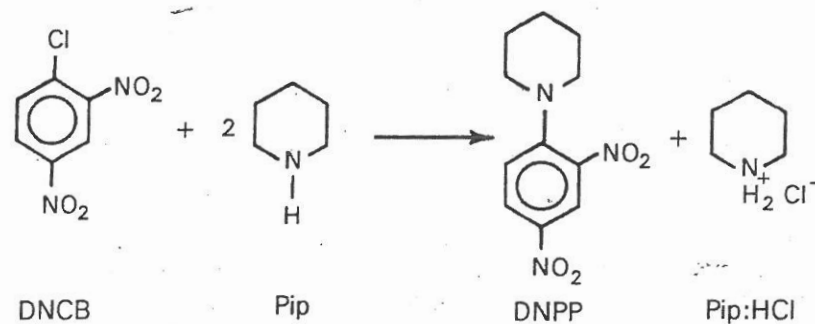
As mentioned previously, the reaction rate is usually temperature-dependent. For many reactions, both in the gas phase and in solution, this dependence can be expressed in terms of the rate constant, $k(T)$:

$$k(T) = A \exp\left(\frac{-E_a}{RT}\right). \quad (5)$$

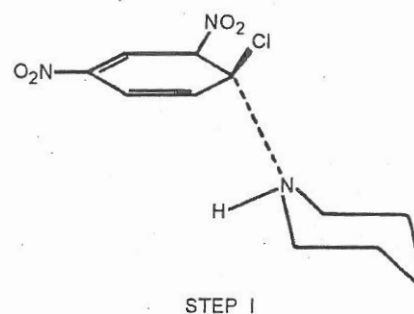
A rate constant whose temperature dependence is accounted for by equation (5) is referred to as an *Arrhenius rate constant*. A is the preexponential, or A -factor, and E_a is the *activation energy*. E_a can be interpreted as the potential energy barrier that must be surmounted in converting reactants to products. This barrier often involves the breaking or rearrangement of chemical bonds, or, in some cases, mass transport through a fluid medium. In the latter case, E_a is much smaller than for a chemical reaction, being approximately equal to E_η , the activation energy to bulk viscous flow.

The Reaction

The reaction that you will study in this experiment involves the coupling of two organic molecules, 2,4-dinitrochlorobenzene (DNCB) and piperidine (Pip). The products of the reaction are 2,4-dinitrophenylpiperidine (DNPP) and piperidine hydrochloride (Pip:HCl). The reaction is shown.

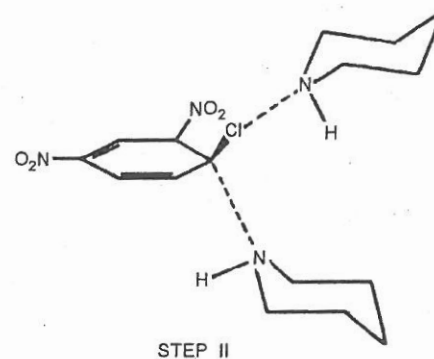


This reaction involves the formation of a nitroaniline derivative that is important in the manufacture of dyes. It has been studied in detail, and the proposed mechanism contains two fundamental, or elementary steps.^{1,2} The first of these involves the nucleophilic attack of the organic base, Pip, on the Cl-bearing C-atom in DNB. This is an example of an S_N2 mechanism in which the intermediate, or transition state, is stabilized by the electron-withdrawing property of the nitro groups, which are ortho and para to the C-Cl site. The Cl atom is thus activated:

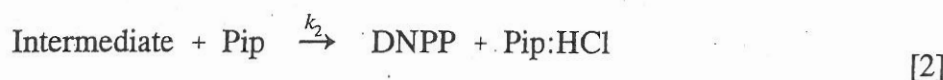
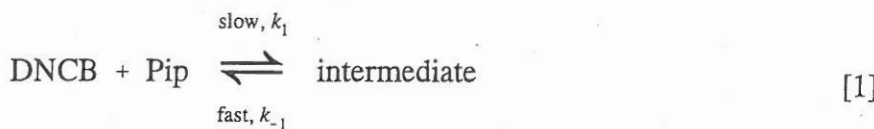


The formation of this intermediate is presumed to take place slowly because of the energy required for the bond rearrangement.

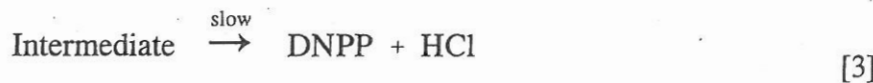
The second elementary step proposed is also bimolecular and involves the participation of another piperidine molecule. In this step, the second piperidine molecule functions simply as an organic base in removing the proton (H⁺) from the piperidine moiety that is being added to the dinitroaryl group.



This two-step mechanism is summarized as follows:



Notice that the intermediate could also decompose unimolecularly to form DNPP and HCl, and the HCl would rapidly react with Pip to form the hydrochloride. Thus, two additional elementary steps might be



We might argue that because piperidine is already in solution in appreciable concentration (to allow step 1 to proceed at a reasonable rate), the rate of the bimolecular product formation step [2] is greater than that of the unimolecular step [3]. If k_2 and k_3 denote the rate constants of these respective steps, the previous statement means that $k_2[\text{Pip}] > k_3$.

By applying the rate determining-step approximation to this mechanism, we can propose that since there is a slow step [1] followed by a fast step that leads to the formation of product [2], the reaction rate is approximately equal to the rate of the slow elementary step. Hence,

$$v = \frac{d[\text{DNPP}]}{dt} \approx k_1 [\text{DNCB}][\text{Pip}] . \quad (6)$$

If $[\text{DNCB}]_0$ and $[\text{Pip}]_0$ represent the initial concentrations of the reactants, and if $[\text{DNPP}]_0 = 0$, it follows from the stoichiometry of the reaction that at an arbitrary time t , the reactant concentrations are

$$[\text{DNCB}]_t = [\text{DNCB}]_0 - [\text{DNPP}]_t ,$$

and

$$[\text{Pip}]_t = [\text{Pip}]_0 - 2[\text{DNPP}]_t . \quad (7)$$

By substituting the time-dependent expressions in equation (7) into the rate law (6) we get a differential equation that is a function of only *one* concentration variable, and the time, namely,

$$\frac{d[\text{DNPP}]}{dt} = k_1 \{[\text{DNCB}]_0 - [\text{DNPP}]\} \{[\text{Pip}]_0 - 2[\text{DNPP}]\} . \quad (8)$$

We can separate the variables to give this *differential rate law*:

$$\frac{d[\text{DNPP}]}{\{[\text{DNCB}]_0 - [\text{DNPP}]\}\{[\text{Pip}]_0 - 2[\text{DNPP}]\}} = k_1 dt . \quad (9)$$

The Integrated Rate Law

The integral on the left-hand side of equation (9) is of standard form, and we can integrate the differential equation subject to the boundary condition $t = 0$; $[\text{DNPP}] = 0$. The result is

$$\ln \left\{ \left(\frac{[\text{DNCB}]_0}{[\text{DNCB}]_0 - [\text{DNPP}]} \right) \left(\frac{[\text{Pip}]_0 - 2[\text{DNPP}]}{[\text{Pip}]_0} \right) \right\} = \{[\text{Pip}]_0 - 2[\text{DNCB}]_0\} k_1 t . \quad (10)$$

This *integrated rate law* appears to be rather complex; that is, the explicit time dependence of $[\text{DNPP}]$ is not of simple form. It is instructive to test this rate law by applying two different experimental stoichiometric constraints. You should realize by now that in studying the reaction experimentally, it is the *concentration of product*, i.e., $[\text{DNPP}]$, that is directly measured as a function of time. We proceed by identifying two limiting conditions.

Condition I

The reactants are stoichiometrically linked. This means that $[Pip]_0 = 2[DNCB]_0$. The significance of this ratio of reactants is that it is valid for *all time* during the reaction, i.e., $[Pip]_t = 2[DNCB]_t$, always. This constraint poses a problem in equation (10a) because of the singularity of the coefficient of the \ln term. If this condition is applied to equation (8), however, the differential equation becomes much simpler, i.e.,

$$\frac{d[DNPP]}{dt} = 2k_1\{[DNCB]_0 - [DNPP]\}^2 \quad (11)$$

This is an example of simple second-order kinetics [rather than mixed second-order, as in equation (8) and equation (11) readily integrates to the familiar form

$$\frac{1}{[DNCB]_0 - [DNPP]} = \frac{1}{[DNCB]_0} + 2k_1 t \quad (12a)$$

$$[DNPP](t) = [DNCB]_0 \left\{ \frac{2[DNCB]_0 k_1 t}{1 + 2[DNCB]_0 k_1 t} \right\} \quad (12b)$$

Condition II

One of the reactants is present in great excess. In this case, we choose $[Pip]_0 \gg [DNCB]_0$; i.e., the system is flooded with piperidine. The constraint kinetically isolates the behavior of the other reactant, DNCB, since there is a negligible decrease in the piperidine concentration with time. Hence, $[Pip]_0 \gg 2[DNPP]$, and thus $[Pip]_t \approx [Pip]_0$. In this case equation (8) becomes

$$\frac{d[DNPP]}{dt} = k_1[Pip]_0\{[DNCB]_0 - [DNPP]\} \quad (13)$$

Integration of this differential equation provides, after rearrangement,

$$\ln \left\{ 1 - \frac{[DNPP]}{[DNCB]_0} \right\} = -\{[Pip]_0 k_1\} t \quad (14a)$$

$$[DNPP](t) = [DNCB]_0 \left\{ 1 - \exp(-[Pip]_0 k_1 t) \right\} \quad (14b)$$

This is an example of a *pseudo-first-order* reaction because the system behaves just as if the formation of product were the result of a first-order process. The quantity $[Pip]_0 k_1$ is not a true constant because it depends on the rather arbitrary value of $[Pip]_0$.

The General Case

But what if experimental conditions pertain in which neither Condition I or Condition II is valid? Then the analysis of the $[DNPP](t)$ data according to equations (12) or (14) would lead to incorrect values of the rate constant k_1 . In this case, the general form of the integrated rate law, equation (10a) applies. That equation can be solved for the explicit time dependence of $[DNPP]$. The result is

$$[DNPP](t) = [DNCB]_0 [Pip]_0 \left(\frac{e^{([Pip]_0 - 2[DNCB]_0)k_1 t} - 1}{[Pip]_0 e^{([Pip]_0 - 2[DNCB]_0)k_1 t} - 2[DNCB]_0} \right). \quad (10b)$$

Equation (10b) is amenable to direct nonlinear regression analysis to obtain k_1 if $[DNPP](t)$ data are available.

The Differential Rate Law

An elegant and, in principle, simple way to escape the sometimes unrealistic (or unachievable) experimental constraints required in Conditions I and II is to analyze the data using the *original* differential rate law, equation (8), which we now express more generally as

$$v = \frac{d[DNPP]}{dt} = k_1 \{ [DNCB]_0 - [DNPP] \}^\alpha \{ [Pip]_0 - 2[DNPP] \}^\beta, \quad (15)$$

where α and β are the (unspecified) reaction orders. If we could obtain the time derivative of the DNPP concentration (i.e., the reaction velocity, v) as a function of $[DNPP]$, we could then carry out a nonlinear regression analysis of the data to obtain the three parameters, α , β , and k_1 . Thus the orders and the rate constant could be obtained directly *without having to make the stoichiometric assumptions of Conditions I and II*.

However, if we were to assume that the reaction orders are both 1, equation (15) simplifies to equation (8), which is a second-order polynomial with only *one* parameter, k_1 . This would allow us to find k_1 very easily from a regression analysis of $d[DNPP]/dt$ vs. $[DNPP]$. Thus, expanding equation (8), we have

$$\frac{d[DNPP]}{dt} = k_1 \{ a[DNPP]^2 + b[DNPP] + c \}, \quad (16)$$

where $a = 2$; $b = -\{[Pip]_0 + 2[DNCB]_0\}$; and $c = [Pip]_0[DNCB]_0$. This experimental approach is described next.

Experimental Method The progress of the reaction could be followed in several ways. One would be to take advantage of the fact that one of the products (Pip:HCl) is an ionic salt and thus to use a conductometric procedure; another would be to titrate the Cl^- ion that is formed. The technique described in this experiment, however, uses a photometric method called *spectrophotometry*. This method is appropriate because although both reactants absorb light

principally in the ultraviolet (DNCB having an absorption maximum at ~ 250 nm), the aniline derivative, DNPP, has an intense absorption peak at 375 nm, which is much closer to the visible region. For this reason, DNPP, in ethanol solution, has a distinct yellow appearance. Absorption spectra of DNCB and DNPP are shown in Figure 1.

The [DNPP] analysis is based on Beer's law, which holds that a linear relationship exists between the absorbance of a species and its molar concentration. The Beer-Lambert law states that

$$A_\lambda = \epsilon_\lambda [\text{DNPP}] l , \quad (17)$$

where ϵ_λ is the *molar absorptivity coefficient* ($\text{dm}^3 \text{ mol}^{-1} \text{ cm}^{-1}$) at the wavelength λ , and l is the optical path length in centimeters. [DNPP] is the molar concentration of the product.

Your first step in this experiment is to obtain a calibration curve of absorbance vs. [DNPP] in order to get a value of ϵ_λ at the appropriate wavelength for the particular experiment carried out.

Two fundamentally different methods can be used to study the kinetics in this experiment. The first involves monitoring the progress of the reaction in *real time* by following the absorbance of the product, DNPP, as a function of time. The second is to *quench* (or stop) the reaction at measured elapsed time intervals after the reactants are mixed ("frozen time").

Method I: Real Time

You will simply add the reactants to a 1-cm absorption cell, mix them rapidly, and immediately place the cell in the (presumably thermostated) compartment of a spectrophotometer. You will monitor the absorbance at an appropriate wavelength as a function of time until the reaction has progressed reasonably far. The data are saved to disk and then subsequently imported to a spreadsheet. Then you will analyze the data numerically, using either an appropriate integrated rate law [equation (12b), (14b), or (10)], depending on the reaction conditions chosen, or the differential rate law [equation (8) or (15)]. These "time scans" may be repeated at different sample conditions (e.g., T). The rate constant, k_1 , and, if desired, the orders α and β , can be found from nonlinear regression analysis. Your spreadsheet must have the capability of performing a numerical differentiation of the absorbance (time) data.

Method II: Frozen Time

In this approach, you will rapidly mix the reactants and allow them to react at a specific temperature. After measured time intervals, you will withdraw samples, rapidly quench them, and then analyze them for DNPP concentration. You must, of course, stop the reaction quickly after withdrawing the sample, otherwise the reaction time will be ambiguous. You do this by immediately adding the withdrawn reaction sample to a quenching solution of aqueous ethanol acidified with sulfuric acid. Once placed in this medium, piperidine is very rapidly protonated, thus making it unreactive, whereupon the reaction is quenched (stopped). You thus determine values of [DNPP] at fixed time points. You then find the rate constant by using the appropriate linearized integrated rate law [equation (12a), (14a), or (10a)].

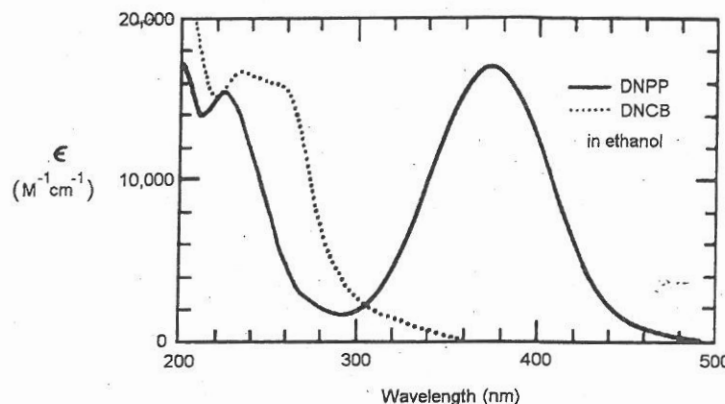


Figure 1. Absorption spectra of starting material, DNBC (...), and product, DNPP (—).

Safety Precautions

- Safety goggles MUST be worn.
- A laboratory coat that covers clothing and arms should be worn.
- Proper pipeting techniques MUST be followed. Never, under any circumstances, pipet by mouth. Consult your instructor if you need help or information about the proper technique.
- CAUTION** This experiment involves the use of solutions of 1-chloro-2,4-dinitrobenzene (DNCB), which is a highly toxic irritant. When handling this material, gloves must be worn. If possible, prepare reaction samples in a fume hood. If any solution comes in contact with the skin, wash immediately with soap and water. Ask your instructor to show you the Material Safety Data Sheet (MSDS) for this and other chemicals encountered in the laboratory.
- CAUTION** Piperidine is a toxic and flammable liquid. It has an objectionable odor; use protective gloves when handling this compound. Work in a fume hood.
- If other reagents or chemicals come into contact with the skin, wash immediately with soap and water.
- Waste material should be deposited in a special, marked container.

Procedure and Data Analysis

REAL-TIME DATA ACQUISITION

Stock solutions of the reactants in absolute ethanol are needed: 0.620 M for Pip and 0.0104 M for DNBC. Data may be acquired for three different stoichiometric, and hence kinetic, conditions: (1) mixed second order [equation (10b)]; (2) simple second order (i.e., $[Pip]_0 = 2[DNCB]_0$) [equation (12b)]; and (3) pseudo first order (e.g., $[Pip]_0 \gg [DNCB]_0$) [equation (14b)]. These equations pertain to the use of the integrated rate laws. One or more of these systems can be studied in this experiment, depending on the time available. In all cases, it is assumed that a stoppered, 1-cm path length, square absorption cell having a capacity of ~ 3 mL is used. For the kinetic runs, a UV-Vis

spectrophotometer is used that is equipped with a thermostated cell holder and that is capable of storing data digitally and providing a text file (ASCII) on a floppy disk. Alternatively any of these kinetic data sets can be analyzed using the differential rate law directly, either equation (15) or (16).

Mixed Second-Order Kinetics

Set the spectrophotometer to a wavelength in the range 470–475 nm. Configure the data acquisition so that a manageable number of points will be acquired in a 45-min scan time. Several hundred points can be easily accommodated by most spreadsheets.

Fill the reference cell with ethanol and place it in the spectrophotometer. Pipet 1.5 mL of the DNB stock solution and 1.5 mL of ethanol into a clean, dry absorption cell. Place this cell in the sample compartment and zero the instrument. Remove the sample cell and start the data acquisition. Inject 100 μ L of the Pip solution into this cell, stopper it, invert it several times, and quickly place it into the spectrophotometer.

Simple Second-Order Kinetics

Follow the same procedure as in (1). Pipet 3.00 mL of the DNB stock solution into the absorption cell. Use this solution to zero the instrument. Remove the sample cell and begin data acquisition. Inject 100 μ L of the Pip solution into this cell. Stopper it, invert it a few times, and quickly place it into the spectrophotometer.

Pseudo-First-Order Kinetics

Set the spectrophotometer to a wavelength in the range 465–470 nm. Use the same procedure for (1). Pipet 0.60 mL of the DNB solution and 2.00 mL of ethanol into the absorption cell. Place it in the sample compartment and zero the instrument. Remove the sample cell and begin data acquisition. Add 0.50 mL (or inject 500 μ L) of the Pip solution, stopper the cell, invert it a few times, and quickly place it into the spectrophotometer.

DNPP Calibration

You will have to obtain the absorptivity coefficient, ϵ , of the DNPP product at the particular analyzing wavelength used (and under the specific bandpass conditions). The value of ϵ at 472 nm is approximately $360 \text{ dm}^3 \text{ mol}^{-1} \text{ cm}^{-1}$. This value can be used if 472 nm is chosen as the analyzing wavelength. If another wavelength is used, or if it is desirable to determine ϵ independently, the absorbance of a known DNPP solution at the desired wavelength must be measured. One possibility is to prepare a solution of Pip and DNB, such as in (3), and to store the mixture in a well-sealed vessel (e.g., a volumetric flask) in the dark for about 1 week. You can then assume that there is a quantitative conversion of the limiting reactant (DNB) to DNPP. Alternatively, you can use an authentic sample of DNPP.

Temperature Dependence

If the activation parameters for the reaction are to be determined, run the reaction associated with one of the preceding protocols using at least three temperatures between ~20 and 60°C. As you would anticipate, significantly less acquisition time is needed for the higher temperatures.

Data Analysis Import the data files into a spreadsheet, and strip off extraneous rows and columns, as necessary. Ultimately you should have two columns of N data points, with, for convenience, column 1 for the time and column 2 for the absorbance values. The first row should correspond to the first "good" absorbance value after the cell was placed in the spectrophotometer. Note that time is not equal to literal zero at that point, but the t values may adjusted to force the first row t to equal 0 for convenience. Next transform the absorbance column to DNPP concentration by dividing by the appropriate absorptivity coefficient.

Analyze using the appropriate integrated rate law [equation (12b), (14b) or (10b)], or one of the differential rate laws [equation (15) or (16)]. In the former case perform nonlinear regression on the $[DNPP](t)$ data. Accordingly, use the explicit time dependence of DNPP as the regression function. However, because the boundary condition $[DNPP] = 0$ for $t = 0$ is not valid for the acquired data (because the beginning of the reaction is not synchronous with data acquisition), you must treat the first $[DNPP]$ value as a regression parameter, or else enter it as a constant (i.e., the *actual* $[DNPP]$ value for the first data point).

For example, if you are analyzing the data acquired under simple second-order conditions, you will fit the data to the following nonlinear function:

$$[DNPP] = [DNPP]_0 + [DNCB]_0 \left(\frac{2[DNCB]_0 k_1 t}{1 + 2[DNCB]_0 k_1 t} \right),$$

in which $[DNCB]_0$ is a known constant, and $[DNPP]_0$ can be "floated" as a regression parameter or otherwise fixed at the observed value for the experimental $t = 0$, and k_1 is, of course, a regression parameter.

In performing nonlinear regression analysis, you must provide an initial value of k_1 . You may estimate this value by examining a plot of the $[DNPP](t)$ data and by approximating the half-life of the reaction, $t_{1/2}$, i.e., the time required to reach half of the limiting DNPP concentration. Depending on the conditions used for the experiment, obtain the initial guess from

$$k_1 \approx \frac{1}{2[DNCB]_0 t_{1/2}} \quad \text{or} \quad \frac{1}{[Pip]_0 t_{1/2}},$$

where the former pertains to simple second-order kinetics and the latter to pseudo first order. In the case of mixed order, i.e., neither first or second, you should use the expression containing the reactant in excess.

If you use the differential rate law, you must first transform the $[DNPP](t)$ data to its derivative. If your spreadsheet does not provide this utility, you may be able to write a simple

procedure to accomplish the objective. Some degree of filtering is highly desirable, and a moving-average method can be employed. An algorithm is presented in the appendix.

The concept is to plot $d[\text{DNPP}]/dt$ vs. [DNPP] and to fit the data to a second-order polynomial using nonlinear regression. Although good results may be obtained directly, it is important to realize that the data in this plot are not rendered in equally spaced [DNPP] values. This condition arises because the value of the derivative decreases with increasing [DNPP]. Thus, there will be few data points early in the reaction (where $d[\text{DNPP}]/dt$ changes rapidly) and many points at long times (where $d[\text{DNPP}]/dt$ changes very slowly). This will have the effect of biasing the analysis in favor of the long-time data points. You can overcome the problem by creating an equally-spaced, or splined transformation of the $d[\text{DNPP}]/dt$ vs. [DNPP] data. A scientific spreadsheet should be able to perform this conversion.

Tabulate the rate constants and their standard deviations obtained at the different temperatures. If you analyzed a given data set using both the integrated and differential rate laws, compare the rate constants (and their standard deviations). Also, compare the results if you carried out the reaction and analyzed the data under two or more different kinetic conditions.

If you obtained rate constants at different temperatures, analyze those results in terms of the Arrhenius expression [equation (5)], and report the activation energy and *A*-factor and their respective standard deviations.

FROZEN-TIME DATA ACQUISITION

Simple Second-Order Kinetics

The following stock solutions will be provided: 0.100 M DNCB and 0.400 M Pip for the reaction, and 0.020 M DNPP for the 460-nm calibration. 50-mL volumetric flasks can be used as reaction vessels.

Initial reactant concentrations of $[\text{DNCB}]_0 = 0.020 \text{ M}$, and $[\text{Pip}]_0 = 0.040 \text{ M}$ will react sufficiently rapidly for a one-laboratory-period experiment.

Prepare and Equilibrate Reactants

1. Add about 30 mL of 95% ethanol solvent and exactly 10 mL of the 0.100 M DNCB solution to each of two 50-mL volumetric flasks. Place each volumetric flask in a different constant-temperature bath (e.g., 0 and 25°C). Keep the other solutions that are to be added to these reactor flasks in their respective temperature baths. Immerse the pipets to be used in the 0°C experiment in 0° ethanol until needed.
2. Place approximately 10 to 20 mL of 0.400 M Pip solution into each of two clean 50-mL volumetric flasks. Next, add about 10 to 20 mL of solvent to each of two other clean 50-mL volumetric flasks. Place one set of these flasks in the 0° bath and the other in the 25° bath. There should then be three flasks in each of the baths. Allow them to equilibrate.
3. While these flasks are equilibrating, label eight 25-mL volumetric flasks (four for each temperature) and fill each with about 15 mL of the quenching solution that is provided. These

flasks do not have to be temperature-equilibrated because the reaction stops as soon as the DNBC/Pip mixtures are added to the acidified ethanol.

460-nm DNPP Calibration

4. Obtain the data for the [DNPP] calibration at 460 nm. You will be shown how to use the spectrophotometer.

Prepare a dilute DNPP solution by pipeting 1 mL of the DNPP stock solution (0.020 M) into a 25-mL volumetric flask; fill to the mark with quenching solution, stopper, and mix. Determine the absorbance at 460 nm.

Set aside three 10-mL volumetric flasks. Pipet into the respective flask 2-, 4-, and 8-mL volumes of the diluted DNPP stock dilution; label each flask. Add quenching solution to each flask up to the mark, stopper, and invert several times. Measure the transmission (or absorbance) of each of these solutions starting with the most dilute. You will use these four readings to construct the 460-nm calibration curve.

Run the Reaction

5. The reaction vessels should be well equilibrated by now. Initiate the reaction by pipetting 5 mL of the temperature-equilibrated Pip solution into the flask containing the DNBC in the 25°C bath. Start the timer (or record the time shown by your watch), immediately add the temperature-equilibrated solvent to the mark, stopper and shake vigorously, and quickly return the reactor flask to the bath. Repeat the procedure for the 0° bath and mark the time at which the Pip was added.

6. Starting with the 25°C sample, remove a 1-mL sample from the reaction mixture as soon as possible and deliver it to one of the 25-mL volumetric flasks containing the quenching solution. Read and record the elapsed time (if you are using a timer, do not shut it off). Do the same for the 0°C reaction. Continue to withdraw 1-mL samples from the reactor vessels, placing them in quenching solution; use (approximately) 5-min intervals for the samples in the 25°C bath and 15-min intervals for the 0°C samples. In all cases, label the samples and record the elapsed times. Obtain at least four "timed" samples for each reaction temperature.

7. As soon as possible after adding a given 1-mL sample to the volumetric flask with the quenching solution, fill the flask to the mark with quenching solution, stopper it, and shake it. Then determine the absorbance at 460 nm.

Pseudo-First-Order Kinetics

In this part of the experiment, you will study the reaction under pseudo-first-order conditions. The methodology is basically identical with that used in Part I. To keep $[Pip] \gg [DNCB]$, the initial DNBC concentration will be much lower than that in Part I, whereas the Pip concentration will be the same. Initial concentrations of $[DNCB]_0 = 5.00 \times 10^{-4}$ M and $[Pip]_0 = 0.040$ M, will be satisfactory.

You will need the following stock solutions: $[DNCB] = 0.010$ M, $[Pip] = 0.400$ M for the reaction, and $[DNPP] = 0.010$ M for the 390-nm calibration.

Prepare and Equilibrate Reactants

1. As before, DNCB, Pip, and solvent samples will be temperature-equilibrated. Pipet 2.5 mL of the 0.010 M DNCB solution into each of two 50-mL volumetric reaction flasks, then add about 40 mL of solvent to each. Add about 15 mL of the 0.400 M Pip solution to two other 50-mL flasks, and about 10 mL of solvent to two other flasks. Place a set of three of these flasks in each temperature bath. Consecutively number eight 10-mL volumetric flasks and add about 5 mL of quenching solution to each. These will receive the reaction samples.

390-nm DNPP Calibration

2. Prepare a 0.4% solution of the 0.010 M DNPP stock solution by first making 10 mL of a 10% (v/v) solution and then using this to make 25 mL of a further 25-fold dilution. Pipette into four clean 10-mL volumetric flasks 1, 2, 3, and 4 mL of the 0.4% DNPP stock solution. Fill each to the mark with quenching solution, stopper, and shake. Measure the absorbances of these four dilutions as well as the 0.4% stock solution at 390 nm. Make sure to set the 100% transmission level using a clean spectrometer cell containing quenching solution.

Run the Reaction

3. Pipet 5 mL of the Pip solution into the DNCB solution in the reaction flask. Start recording the time. Immediately fill the flask with temperature-equilibrated solvent, stopper it and shake it thoroughly, and then replace it in the bath. Do likewise for the 0°C sample; be sure to use the 0°-equilibrated pipet for delivering the Pip solution.

4. Quickly withdraw a 1-mL sample from each reaction flask, starting with the 25°C sample, and add it to one of the 10-mL flasks containing quenching solution.

5. Continue to withdraw 1-mL samples from the reaction flasks, adding the samples to quenching solution and preparing 10-mL analysis samples. Withdraw samples from the 25°C reaction vessel approximately every 2½ min, and from the 0°C reaction every 15 min. Obtain a total of at least four “timed” samples for each reaction.

6. Measure the absorbance of the samples at 390 nm. Make sure to zero the spectrophotometer for a sample cell filled with pure quenching solution.

Data Analysis and Calculations

1. Tabulate the [DNPP] calibration data obtained at 460 and 390 nm; these consist of absorbance and [DNPP] values. For each wavelength, plot absorbance vs. [DNPP] and obtain the least-squares values of ϵ . These plots should pass through the origin; use a linear regression program that constrains the y-intercept to 0. Knowing the path length of the absorption cells, report the molar absorptivity coefficients at 460 and 390 nm. Note that the actual ϵ values measured depend on the spectrophotometer bandpass used and thus may not agree exactly with the spectra shown in Figure 1.

2. Tabulate the {absorbance,time} data for the 0 and 25°C reactions for Parts I and II. Using the ϵ values obtained from the calibration curves, convert the absorbances into [DNPP] and enter these concentrations in the same table.
3. Using the appropriate dilution factor, transform the analyzed [DNPP] values into those pertinent to the reaction conditions. Then determine $\{[DNCB]_0 - [DNPP]\}$ and tabulate with the reaction times.
4. For the Part I data, prepare plots according to equation (12a) and obtain the linear regression slopes, and from these, determine k_1 at 0 and 25°C. Likewise, analyze the data in Part II according to equation (14a) and obtain the least-squares values of the pseudo-first-order rate constants, and from them determine k_1 at 0 and 25°C.
5. From the two rate constants at the two temperatures, estimate the activation energy and frequency factor for the reaction.
6. Compare the values of k_1 obtained from Parts I and II (at each temperature). Comment on any discrepancies.

Questions and Further Thoughts

1. Another approach to the analysis of the mechanism described here is to apply the steady-state approximation to the intermediate. Show that this approach gives equation (6) under conditions where $k_2[\text{Pip}] \ll k_{-1}$.
2. Indicate the expected reaction order if $k_2[\text{Pip}] \ll k_{-1}$. Derive the modified equation appropriate to conditions I and II under this circumstance and suggest which forms can be plotted to give a linear result.
3. Considering the structure of the proposed intermediate (see Step I), and its decomposition into the product (see Step II), what would the effect on the reaction rate be if a secondary amine such as di(*t*-butyl)amine was used? Explain.
4. The stability of the intermediate can be considered in terms of two simple factors: steric bulkiness of the amine, and its electron-donating ability. How does each of these factors affect the rate of reaction? Suggest amines that would allow these factors to be "varied" experimentally (as independently as possible).
5. Transition-state theory allows a rate constant to be expressed in terms of the thermodynamic parameters activation entropy (ΔS^\ddagger) and activation enthalpy (ΔH^\ddagger). For a second-order reaction in solution, the rate constant can be expressed as

$$k = \frac{k_B T}{h} \exp\left(\frac{\Delta S^\ddagger}{R}\right) \exp\left(-\frac{\Delta H^\ddagger}{RT}\right),$$

where k_B is the Boltzmann constant and h is Planck's constant, T is the absolute temperature, and ΔH^\ddagger can be written in terms of E_a , the Arrhenius activation energy [see equation (5)]: $\Delta H^\ddagger = E_a - RT$. Using your values of the second-order rate constant at 298 K and the activation energy, determine the entropy and enthalpy of activation for the reaction.

6. Show that in the limit $t \rightarrow \infty$, $[DNPP] \rightarrow [DNCB]_0$ if DNB is the limiting reagent, and $[DNPP] \rightarrow [\text{Pip}]_0/2$ if Pip is the limiting reagent.

Notes

1. O. L. Brody and F. R. Cropper, *J. Chem. Soc.*, 1950:507 (1950).
2. J. F. Bunnett and H. D. Crockford, *J. Chem. Educ.*, 33:552, (1956).

Further Readings

- R. A. Alberty and R. J. Silbey, *Physical Chemistry*, pp. 624–732, Wiley (New York), 1997.
P. W. Atkins, *Physical Chemistry*, 5th ed., pp. 861–887, W. H. Freeman (New York), 1994.
I. N. Levine, *Physical Chemistry*, 4th ed., pp. 493–549, McGraw-Hill (New York), 1995.
J. H. Noggle, *Physical Chemistry*, 3d ed., pp. 501–530, HarperCollins (New York), 1996.
B. B. Ramachandran and A. M. Halpern, *J. Chem. Educ.*, 73:686, (1996).

Experiment 21

Data Sheet A (Page 1)

Kinetics of a Homogeneous Reaction

NAME _____

DATE _____

Real-Time Method

Concentrations of Reactants:

Temperature _____

Data-Acquisition Parameters

Frozen-Time Method, Part I

Second-Order Kinetics

Calibration at 460 nm:

Concentration Absorbance

_____	_____
_____	_____
_____	_____
_____	_____
_____	_____

Experiment 21

Data Sheet A (Page 2)

Kinetics of a Homogeneous Reaction

NAME _____ DATE _____

Time, min Absorbance, 460 nm Time, min Absorbance, 460 nm

_____	_____	_____	_____
_____	_____	_____	_____
_____	_____	_____	_____
_____	_____	_____	_____
_____	_____	_____	_____
_____	_____	_____	_____
_____	_____	_____	_____
_____	_____	_____	_____

Frozen-Time Method, Part II

Pseudo-First-Order Kinetics

Calibration at 390 nm:

Concentration Absorbance

t_∞ data:

Absorbance at 460 nm _____

Absorbance at 390 nm _____

Temperature = 0°C

Temperature = _____

Time, min Absorbance, 390 nm

Time, min Absorbance, 390 nm

_____	_____
_____	_____
_____	_____
_____	_____
_____	_____
_____	_____
_____	_____
_____	_____

_____	_____
_____	_____
_____	_____
_____	_____
_____	_____
_____	_____
_____	_____
_____	_____

Experiment 21

Data Sheet B (Page 1)

Kinetics of a Homogeneous Reaction

NAME _____

DATE _____

Real-Time Method

Concentrations of Reactants:

Temperature _____

Data-Acquisition Parameters

Frozen-Time Method, Part I

Second-Order Kinetics

Calibration at 460 nm:

Concentration Absorbance

_____	_____
_____	_____
_____	_____
_____	_____
_____	_____

Experiment 21**Data Sheet B (Page 2)****Kinetics of a Homogeneous Reaction**

NAME _____

DATE _____

Time, min Absorbance, 460 nm

Time, min Absorbance, 460 nm

_____	_____
_____	_____
_____	_____
_____	_____
_____	_____
_____	_____
_____	_____

_____	_____
_____	_____
_____	_____
_____	_____
_____	_____
_____	_____
_____	_____

Frozen-Time Method, Part II**Pseudo-First-Order Kinetics**

Calibration at 390 nm:

Concentration Absorbance

_____	_____
_____	_____
_____	_____
_____	_____
_____	_____

 t_{∞} data:

Absorbance at 460 nm _____

Absorbance at 390 nm _____

Temperature = 0°C

Temperature = _____

Time, min Absorbance, 390 nm

Time, min Absorbance, 390 nm

_____	_____
_____	_____
_____	_____
_____	_____
_____	_____
_____	_____
_____	_____

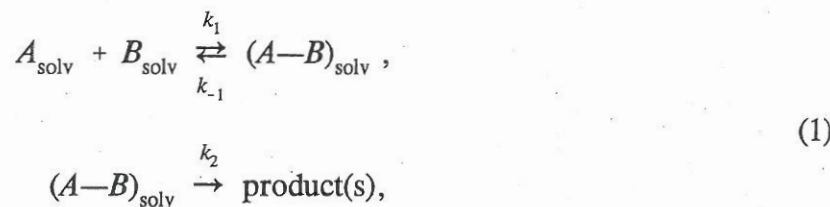
_____	_____
_____	_____
_____	_____
_____	_____
_____	_____
_____	_____
_____	_____

Experiment 22

The Kinetics of a Diffusion-Controlled Reaction

Objective To determine the rate constant and collision diameter of a diffusion-controlled reaction (photoexcited anthracene with carbon tetrabromide) using the technique of fluorescence quenching.

Introduction In this experiment you will study a very fast bimolecular reaction between two different species in solution. Let us assume that the reactants, *A* and *B*, which are electrically neutral, undergo independent, random motion in solution. There is a certain probability that *A* and *B* will encounter each other at some close distance, *R*, where *R* is approximately equal to the sum of their molecular radii. This arrangement is called an *encounter complex*. Because there is a tendency for the solutes *A* and *B* to maintain constant random motion, it is inevitable that, once loosely held in this complex, they will subsequently separate from each other unless a chemical reaction (or other definitive process) first links them together or causes them to react. Since this random motion takes place in a "bath" of solvent molecules (assumed to be unreactive with respect to *A* and *B*), the separation of the *A*—*B* encounter complex will be impeded by the neighboring solvent molecules. This artificial holding together of the two molecules is called the *cage effect*. The important point is that there is a kinetic competition between a net (thus measurable) reaction between *A* and *B* via the collision complex, and the release of *A* and *B* from the solvent cage back into the solvent medium where no reaction occurs. We can represent these processes by the following kinetic scheme:



where A_{solv} and B_{solv} represent the solvated *A* and *B* molecules, and $(A-B)_{\text{solv}}$ is the solvated encounter complex. The rate constants for these elementary steps are denoted as k_1 , for the bimolecular formation of the encounter complex (or diffusion into the solvent cage); k_{-1} , for the unimolecular dissociation of the complex (or diffusion out of the solvent cage); and k_2 for the "unimolecular" reaction between *A* and *B* in the complex to form the product(s).

Because we assume that the encounter complex undergoes rapid deactivation, either by dissociation or via reaction, we can employ the steady-state approximation, according to which the net formation rate of $(A-B)_{\text{solv}}$ is zero. Thus

$$\frac{d[A-B]}{dt} = k_1[A][B] - (k_{-1} + k_2)[A-B] = 0,$$

and we can approximate the steady-state concentration of the encounter complex as

$$[A-B] \approx \frac{k_1[A][B]}{k_{-1} + k_2}$$

Now, if we further assume that the reaction rate is given by the slow step, i.e., $k_2[A-B]$, we can express that rate as

$$\text{Rate} \approx k_1 k_2 [A-B] = \frac{k_1 k_2}{k_{-1} + k_2} [A][B]$$

For convenience, we define the second-order rate coefficient, k_{obs} , as

$$k_{\text{obs}} \equiv \frac{k_1 k_2}{k_{-1} + k_2} \quad (2)$$

This analysis leads to two limiting cases with respect to k_{obs} : (1) The reaction between A and B is very slow compared with their departure (and separation) from the solvent cage, i.e., $k_{-1} \gg k_2$; and (2) the $A-B$ reaction is much faster than their separation, or $k_2 \gg k_{-1}$. The first case describes a reaction that is under *chemical control*, with $k_{\text{obs}} \approx k_1 k_2 / k_{-1}$, and the second pertains to a *diffusion-controlled* reaction for which $k_{\text{obs}} \approx k_1$. The latter situation is considered in this experiment. More details of the reaction, which involves fluorescence quenching, will be described after a discussion of the relevant theoretical ideas.

Diffusional Mass Transport

The basic issue in a diffusion-controlled reaction concerns the dynamics of mass transport in the condensed phase. The fundamental equations describing mass transport are embodied by Fick's laws of diffusion. These laws are also encountered and discussed in Experiment 19. Fick's first law says that the number of molecules, dn , diffusing through a unit area, A , per unit time, dt , in the x -direction (i.e., the flux, J_x) is proportional to the concentration gradient at that point, i.e.,

$$J_x \equiv \frac{1}{A} \frac{dn}{dt} = -D \frac{dC}{dx}, \quad (3)$$

where the proportionality constant D is called the *diffusion coefficient*. The cgs units of D are $\text{cm}^2 \text{s}^{-1}$. The minus sign in equation (3) indicates that transport goes *against* the concentration gradient (i.e., from high to low concentration values).

Fick's second law states that the change in the concentration of molecules, dC , diffusing across an infinitesimally thin plane per unit time, dt , is proportional to the gradient of the flux:

$$\left(\frac{dC}{dt} \right)_x = - \left(\frac{dJ_x}{dx} \right)_t . \quad (4)$$

Again, the minus sign ensures that concentration increases in time in response to a flux that decreases with increasing x . If we assume D to be independent of x , we may substitute the expression for J_x from Fick's first law into the second to give

$$\left(\frac{dC}{dt} \right)_x = D \left(\frac{d^2 C}{dx^2} \right)_t . \quad (5)$$

Because we are concerned with a three-dimensional and isotropic space, i.e., equal forces in all directions, we can write Fick's second law in more general form as

$$\left(\frac{dC}{dt} \right)_{x,y,z} = D (\nabla^2 C)_t , \quad (6)$$

where ∇^2 is the Laplacian operator $\partial^2/\partial x^2 + \partial^2/\partial y^2 + \partial^2/\partial z^2$.

The solution of Fick's second law is an equation that expresses concentration as a function of *space*, i.e., distance, r , and *time*, t . We are interested in solving equation (6) with the boundary conditions

$$\begin{aligned} C(r, 0) &= C_0, \\ C(\infty, t) &= C_0, \\ C(r = R, t) &= 0, \end{aligned}$$

where $r = [x^2 + y^2 + z^2]^{1/2}$, and C_0 denotes the *bulk* concentration.

The first boundary condition states that initially the bulk concentration prevails throughout the system; the second says that even after the reaction starts ($t > 0$), the concentration very far away from the reactant is constant, i.e., the bulk concentration, C_0 ; and the third indicates that the reactant concentration is zero at a distance equal to the sum of the reactant collision radii. Note that the diffusion coefficient, D , contained in equations (3), (5), and (6) is the *sum* of the individual diffusion coefficients of the reactants, $D_A + D_B$. This expression essentially allows the motion of one of the reactants to be considered *relative* to the other.

The solution of Fick's second law for this set of boundary conditions (first rendered by Smoluchowski in 1917) yields, for the space-time dependence of C ,

$$C(r, t) = C_0 \left\{ 1 - \frac{R}{r} \operatorname{erfc} \left[\frac{(r-R)}{2} (Dt)^{1/2} \right] \right\} , \quad (7)$$

in which erfc is the *co-error function*,

$$\operatorname{erfc}(x) \equiv 1 - \frac{2}{\pi} \int_0^x \exp(-y^2) dy .$$

The time dependence of reactant at the reaction boundary $r = R$ becomes expressible in terms of the flux of reactant, J_R , or its rate of transport across a hypothetical spherical surface with radius R . Thus

$$J_R = \frac{4\pi RDN_A C_0}{1000} \left[1 + \frac{R}{(\pi Dt)^{1/2}} \right] \text{ molecules s}^{-1}, \quad (8)$$

where N_A is Avogadro's number. Equation (8) indicates that the flux (molecules per unit area per second) is actually time-dependent. This time dependence comes from $R/(\pi Dt)^{1/2}$, which is sometimes referred to as the *transient term*. Physically, the transient term accounts for the fact that initially nearby reactant molecules do not have to diffuse through the bulk medium in order to react. After a short time, however, these nearby reactant molecules are depleted, and the flux approaches a constant, or steady-state, value, $4\pi RDN_A C_0/1000$. This can be seen mathematically in that time is represented in equation (8) as $t^{1/2}$.

Because J_R represents the rate of passage of one of the reactants (having a bulk concentration C_0 in mol dm^{-3}) through a spherical reaction surface with the other reactant at the center, the rate of the reaction represented by equation (1) is merely J_R itself. Hence, the bimolecular, diffusion-controlled rate constant k_1 is J_R/C_0 ,

$$k_1 = \frac{4\pi RD}{1000} \left[1 + \frac{R}{(\pi Dt)^{1/2}} \right] (\text{dm}^3 \text{ mol}^{-1} \text{ s}^{-1}). \quad (9)$$

The units shown pertain if R and D are expressed in cm and $\text{cm}^2 \text{ s}^{-1}$, respectively. This rate constant is not a true *constant*, however, because of the transient term. However, as t becomes large enough,

$$k_1 \rightarrow \frac{4\pi RD}{1000} (\text{dm}^3 \text{ mol}^{-1} \text{ s}^{-1}), \quad (10)$$

and equation (10) can be used to determine the diffusion-controlled rate constant if the mutual diffusion constant ($D_A + D_B$) and collision radii ($R_A + R_B$) are known. We emphasize again that the units of k_1 presented above are $\text{dm}^3 \text{ mol}^{-1} \text{ s}^{-1}$, if R and D are expressed in cm and $\text{cm}^2 \text{ s}^{-1}$, respectively.

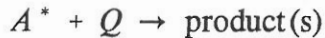
Often, however, R and D are not known, and an indirect method is used to estimate k_1 . This approach, developed by Einstein using Stokes's law (see Experiment 17), allows the diffusion coefficient to be expressed in terms of a *bulk property*, the solvent viscosity, η . Thus

$$k \approx \frac{8RT}{3000\eta} \quad (\text{dm}^3 \text{ mol}^{-1} \text{ s}^{-1}), \quad (11)$$

where R is the gas constant. Equation (11), which is often referred to as the Stokes-Einstein-Smoluchowski (SES) equation, holds when the reactants A and B are different and their sizes are larger than that of the solvent molecules. The indicated units are obtained if R and η are expressed in cgs units, i.e., $8.314 \times 10^7 \text{ erg mol}^{-1} \text{ K}^{-1}$ and poise, respectively.

Fluorescence Quenching

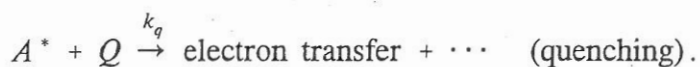
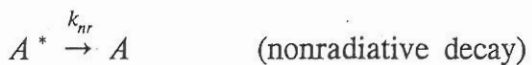
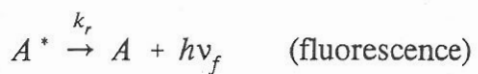
The reaction studied in this experiment takes place between an electronically excited molecule and a quencher, a species that removes the electronic excitation. The advantages of using an electronically excited molecule as one of the reactants are: (1) the reaction takes place only when the system is exposed to light; (2) the concentration of electronically excited molecules can be readily followed fluorimetrically (via fluorescence detection); and (3) the reaction itself is intrinsically fast: It has no activation energy per se, and is limited by the encounter between the excited molecule and the quencher. Experiments 27, 29, 31 and 35 also utilize luminescence quenching as a "kinetic" technique. The overall reaction describing fluorescence quenching can be represented as



where A^* represents the electronically excited (fluorescent) state of a molecule (e.g., anthracene in this experiment), Q denotes the quencher (e.g., CBr_4) that "extinguishes" the A^* fluorescence, and "product(s)" indicates the species into which the fluorescent molecule is eventually transformed. This deexcitation process may occur through a charge-transfer intermediate ($A^+ - Q^-$) in which electronic charge is transferred to the quencher molecule from the excited-state species. For the system encountered in this experiment, electron transfer from A^* to the quencher occurs very rapidly. In general, it is possible that the consequence of fluorescence quenching is the return of A to its electronic ground state without any change in structure, i.e., $A + Q$.

In the case of CBr_4 , the quenching mechanism involves the electron transfer from the excited state, A^* , to CBr_4 , which is more electronegative than A^* . A reverse electron transfer then restores the two molecules to their neutral species, A being in the ground state. (See Experiment 27 for another example of quenching via electron transfer.)

The bimolecular quenching reaction shown above, however, competes with the intrinsic first-order fluorescence decay of A^* and thus reduces the probability that the A^* species will emit a photon. A more complete scheme is thus



If a solution containing A and Q is irradiated with a *steady-state* light source (at a wavelength where A absorbs), a very small time-independent concentration of A^* is produced. The probability that A^* will fluoresce, P_f , is the ratio of the fluorescence (or radiative) rate constant to the sum of all the rate constants that deplete A^* , namely,

$$P_f = \frac{k_r}{k_r + k_{nr} + k_q[Q]}, \quad (12)$$

where k_r , k_{nr} , and $k_q[Q]$ are, respectively, the radiative, nonradiative, and (pseudo-first-order) quenching rate constants. Since $[Q] >> [A^*]$, the diffusion-controlled bimolecular quenching step becomes pseudo first order. If the amount of light absorbed by A is unaffected by $[Q]$, the fluorescence intensity, I , measured by the detector (i.e., the instrument response) is proportional to P_f . In the absence of quencher, $I = I_0 = k_r/(k_r + k_{nr})$, and the ratio of fluorescence intensities of unquenched to quenched samples of A becomes

$$\frac{I_0}{I} = 1 + \frac{k_q[Q]}{k_r + k_{nr}}. \quad (13)$$

Identifying $1/(k_r + k_{nr})$ as the reciprocal of the *fluorescence lifetime* of A^* in the absence of quencher (τ_0), we can write equation (13) as

$$\frac{I_0}{I} - 1 = k_q \tau_0 [Q]. \quad (14)$$

Equation (14) is known as the steady-state *Stern-Volmer* (S-V) relation as applied to fluorescence quenching. It predicts that a plot of $(I_0/I - 1)$ vs. $[Q]$ should be linear, having an intercept of zero and a slope equal to $k_q\tau_0$. (See also Experiments 27, 29, and 35.) The latter is called the Stern-Volmer constant, K_{sv} (units of $\text{dm}^3 \text{ mol}^{-1}$). If fluorescence quenching is diffusion-controlled (which is the case in the anthracene/CBr₄ system), k_q can be identified with k_1 [see equations (1), (2) and (9-11)].

In the absence of the transient effect, which is a type of "static" quenching in that some A^* molecules are quenched by nearby Q molecules that do not have to undergo transport fully through the solvent medium in order to approach A^* within a distance R , the S-V plot should be linear, and independent knowledge of τ_0 allows us to determine k_q . Alternatively, if the process is known to be diffusion-controlled, and if k_1 is determined from the SES (or some other) equation [e.g., equation (10)], the fluorescence lifetime of A^* can be estimated from the measured K_{sv} value. This is a case in which a dynamic property (a rate constant) can be obtained from a static experiment (I_0/I measurements).

The S-V relation can be expressed in terms of the diffusion-controlled rate constant that contains the transient term, e.g., equation (9). The time dependence was treated by Ware and Novros, who applied equation (9) to the condition pertinent to this experiment, namely, that the system is considered to be suddenly exposed to a steady-state excitation source, called a step function (see Figure 1 and *Further Readings*). In this case, the S-V equation becomes more complicated:

$$\frac{I_0}{I} = \frac{1 + 4\pi RDN_A/\{1000[Q]\tau_0\}}{Y}, \quad (15)$$

where

$$Y = 1 - \frac{b}{a^{1/2}} \exp\left(\frac{b^2}{a}\right) \operatorname{erfc}\left(\frac{b}{a^{1/2}}\right), \quad (16)$$

in which

$$a = \frac{1}{\tau_0} + \frac{4\pi RDN_A}{1000[Q]},$$

$$b = \frac{4R^2(\pi D)^{1/2}N_A}{1000[Q]}.$$

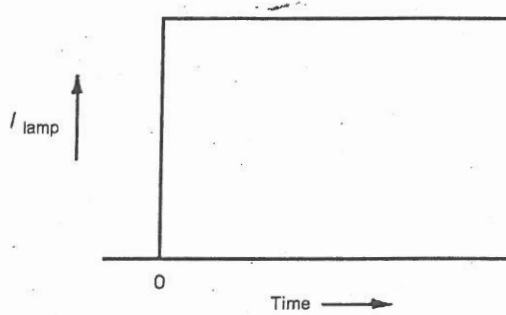


Figure 1. Step excitation function. At time = 0, absorbing radiation is suddenly “switched on.”

If $Y = 1$, equation (15) reduces to equation (14), in which case $k_q = k_1$ from equation (10). (Verify this!)

The Stern-Volmer plot based on equation (15) will be curved upward. If the mutual diffusion coefficient of the reacting pair is known, the S-V plot of experimental data can be fit using equation (15) with R used as a “fitting” parameter. For a satisfactory match between experiment and theory, however, the value of R must be physically reasonable. That is, R should be approximately equal to the sum of the molecular diameters of A (actually A^*) and Q .

Safety Precautions

- Always wear safety glasses or goggles; these glasses should block ultraviolet light. Ordinary plastic safety goggles or glasses may not be effective in absorbing all the ultraviolet radiation. Check with your instructor.
- Do not allow solid anthracene to come in contact with the skin. Wear gloves when handling anthracene and CBr_4 .
- Ozone is sometimes produced by ultraviolet light sources. If you detect this gas, which has a sharp, slightly acrid odor, notify your instructor and immediately shut off the source. Increase ventilation, and leave the room immediately.
- The compressed-gas cylinder used in deaerating should be securely strapped to a firm support. The delivery pressure should never exceed a few (e.g., 5) psig.
- The experiment should be performed in an open, well-ventilated laboratory.

Procedure

1. Using freshly sublimed or purified anthracene and CBr_4 , prepare 250 mL of an $\sim 1.00 \times 10^{-4}$ M solution of anthracene (AN) in spectrometric (or fluorometric) quality *n*-hexane. Using this solution as “solvent,” prepare 25 mL of an $\sim 1.50 \times 10^{-2}$ M “stock” solution of CBr_4 .
2. Prepare at least eight dilutions of the AN/ CBr_4 stock solution using the AN solution as solvent. The most dilute should be 5%, and the rest should be nearly evenly spaced up to the stock-solution value. 10-mL volumes of each solution are appropriate. Include 0 and 100% samples for uniformity. Label these samples.

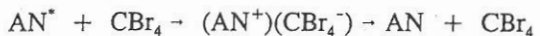
3. Starting with the 0% sample (AN only), introduce the solution into a fluorescence cell and deaerate with dry N₂ for about 2 min. Avoid using an excessive flow rate that will cause the solution to splatter from the cell or to otherwise result in undue solvent evaporation. Promptly stopper the cell.
4. Record the full fluorescence spectrum using the instrumental conditions previously outlined by the instructor. Label the spectrum while it is being recorded (if a strip-chart recorder is used).
5. Using exactly the same excitation wavelength as in step 4, measure the fluorescence intensity of the most dilute and subsequently more concentrated AN/CBr₄ solutions. You must deaerate each sample in a consistent procedure (i.e., identical bubbling time). However, instead of obtaining the entire fluorescence spectrum, you need monitor only the AN maximum (near ~398 nm). Make sure you are at the maximum by first scanning that region slowly. If you have any doubt as to the steadiness of the exciting source, switch back to the AN sample and compare its maximum intensity with that of the first sample run.
6. As you examine increasingly more concentrated samples are examined, the fluorescence intensity will diminish to the point that you will need to increase the instrument gain (i.e. signal amplification) to ensure maximal reading sensitivity. Establish the background, or "dark check," when the instrument sensitivity is changed.
7. Keep in mind the following procedural points: (a) The temperature of the sample should be held constant to 0.5 to 1°C; (b) the exposure times of all of the samples (especially those rich in CBr₄) to the excitation source (and even room light) should be minimized; and (c) samples should be stored in the dark until they are used.

Data Analysis

1. Tabulate the data as I_f (AN fluorescence intensity), and [Q] (CBr₄ concentration), or enter the data into a spreadsheet.
2. Make a Stern-Volmer plot of the data.
3. Superimpose on this plot the straight line expected if the transient term is ignored. The following information can be used: Ware and Novros reported a value of $D = 4.35 \times 10^{-5} \text{ cm}^2 \text{ s}^{-1}$ in *n*-heptane at 25°C. To obtain D for *n*-hexane at some other temperature, assume that D is proportional to T/η . They also reported a value of $\tau_0 = 5.52 \times 10^{-9} \text{ s}$. You can assume this to be temperature-independent.
4. Also indicate the straight line expected on the basis of the SES equation. Tabulate the two calculated k_1 values and their error limits.
5. Using equation (15), calculate several points for the S-V plot using a fixed value of R . If you are not using a computer to generate these points, choose them judiciously so you can discern the general shape of the calculated plot. Start with a value of 6 Å and increase R in steps of 0.5 Å until you obtain satisfactory agreement with the data.

Questions and Further Thoughts

1. Why is the anthracene fluorescence quenching diffusion controlled, as opposed to chemical controlled? Thus justify why the reaction between AN^* and CBr_4 is very fast.
2. What experiment(s) could you perform to determine whether a stable photoproduct is formed as a result of the fluorescence quenching?
3. What could you do to obtain supporting evidence for the existence of a charge-transfer (or ion-pair) intermediate, e.g.,



in the quenching process?

4. Verify that if $Y = 1$ in equation (15), $k_q \sim k_1$; see equations (14) and (10).
5. One of the undesirable complications associated with this type of experiment is the potential presence of *ground-state* complexes between AN and CBr_4 . If such a complex competes for light absorption with uncomplexed, free anthracene, it can cause a decrease in fluorescence intensity without there having to be a diffusion between AN^* and CBr_4 . This is sometimes called *static quenching*. For this reason, it is desirable to work with quencher concentrations as low as possible. What experiment could you do to obtain evidence of a ground-state complex? How could you determine the equilibrium constant of such a complex?
6. What effect would a polar solvent, e.g., acetonitrile (CH_3CN), have on the ground- and excited-state interactions between AN and CBr_4 ?
7. If you wanted to do a fluorescence quenching experiment that demonstrated (and thus maximized) the transient effect in diffusional processes, what qualities of solvent viscosity and fluorescence probe lifetime would you seek (i.e., high or low viscosity; long or short fluorescence lifetime)?
8. The lowering of dissolved oxygen by bubbling the solution with dry N_2 gas (deairating) is an application of Henry's law. Explain how deaeration works in this context.

Further Readings

- R. A. Albery and R. J. Silbey, *Physical Chemistry*, 2d ed., pp. 692–696, Wiley (New York), 1997.
 A. H. Alwattar, M. D. Lumb, and J. B. Birks, *Organic Molecular Photophysics*, vol. 1, p. 403, Wiley (New York), 1973.
 P. W. Atkins, *Physical Chemistry*, 5th ed., p. 795, W. H. Freeman (New York), 1994.
 I. N. Levine, *Physical Chemistry*, 4th ed., p. 469, McGraw-Hill (New York), 1995.
 J. H. Noggle, *Physical Chemistry*, 3d ed., p. 480, HarperCollins (New York), 1996.
 J. B. Birks, *Photophysics of Aromatic Molecules*, p. 518, Wiley (New York), 1970.
 R. M. Noyes, *Progress in Reaction Kinetics*, vol. 1, 131 (1961).
 N. J. Turro, *Modern Molecular Photochemistry*, p. 311, Benjamin-Cummings (Menlo Park, Calif.), 1978.
 W. R. Ware and J. S. Novros, *J. Phys. Chem.*, 70:3246 (1966).

Experiment 22

Data Sheet A

Diffusion-Controlled Rate Constant

NAME _____

DATE _____

Anthracene concentration: _____ g in _____ mL

CBr₄ stock solution: _____ g added

AN/CBr₄ Solutions
% stock

Fluorescence Intensity

Temperature: _____

0%

Experiment 22

Data Sheet B

Diffusion-Controlled Rate Constant

NAME _____

DATE _____

Anthracene concentration: _____ g in _____ mL

CBr₄ stock solution: _____ g added

AN/CBr₄ Solutions
% stock

Fluorescence Intensity

Temperature: _____

0%

Transport Properties and Chemical Kinetics

8

Experiment 17

Viscosity of Liquids Part I: Low Viscosities

Objective To measure and analyze the viscosities of ideal (toluene/*p*-xylene) and nonideal (methanol/water) binary solutions and their components; to determine the activation energy to viscous flow.

Introduction From a phenomenological point of view, we can say that the viscosity of a fluid is its resistance to flow. Viscosity measurements are often carried out for either of two main reasons. Viscosity is a quantitative property of a fluid and although a particular sample might be highly complex, such as a blend of various resins or polymers, its viscosity serves to represent a physical property of that system. Viscosity therefore can be used as an empirical index in quality-control applications concerning, for example, oils and resins, latex paints, or chocolate mousse. Another motivation for measuring viscosity is to determine a fundamental and intrinsic property of a liquid (as a solvent medium): the rate of mass transport, or diffusion, within the medium. In this application, for example, viscosity data can provide important information about chemical reaction kinetics. In this experiment, the fluid will be either a pure liquid or a mixture of liquids.

Considered macroscopically, viscosity is a frictional force that arises from the directed motion of molecules past each other in the liquid state. From a microscopic viewpoint, viscosity reflects the energetics of molecular association in the liquid state because in order for a liquid to flow, a force must be applied to overcome the attractive forces between the molecules. These forces are appreciable; they are manifest, for example, as latent heat of vaporization and surface tension. The mathematical treatment of viscosity is best introduced by looking at Figure 1.

A liquid is presumed to be flowing smoothly in the *x*-direction. Imagine that the liquid is composed of sheets of infinitesimal cross section *dA* that are oriented in the *x*-*y* plane, and that each sheet flows tangentially to its surface area, in the positive *x*-direction. If a given sheet is kept at a velocity v_x such that it exceeds the velocity of an adjacent sheet by an amount dv_x and the adjacent sheet is displaced by a distance *dz* the force required (per unit area) to maintain the motion of the given sheet, df_x , is given by

$$\frac{df_x}{dA} = \eta \left(\frac{\partial v_x}{\partial z} \right)_z \quad (1)$$

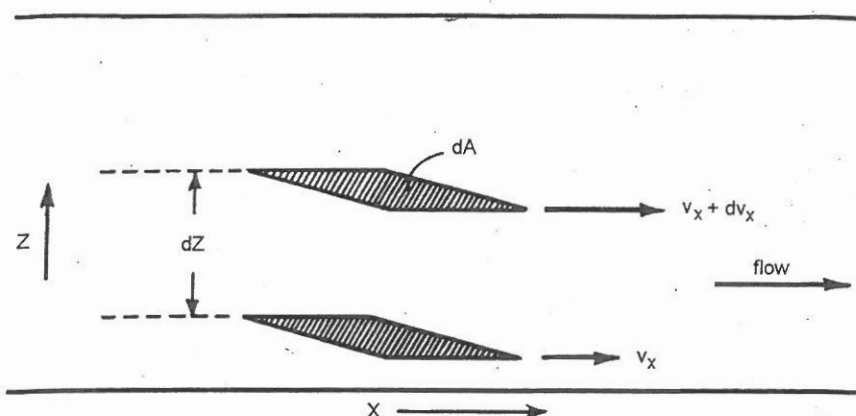


Figure 1. In viscous flow, a sheet of fluid having cross-sectional area dA is subjected to a force that causes it to move faster by an amount dV than an equivalent, adjacent sheet separated by a distance dz . The planes of the sheets are normal to the flow direction.

The partial derivative, $(\partial v_x / \partial z)_z$, is the tangential velocity gradient, and η , the proportionality constant between f_x and this gradient, is now defined as the *viscosity coefficient*. From equation (1), it can be seen that the SI dimensions of the viscosity coefficient are $\text{kg m}^{-1} \text{ s}^{-1}$. Equation (1) is called Newton's law of viscous flow. Fluids that behave according to (1) are called Newtonian fluids and are said to undergo *laminar* flow. Cases of nonlaminar, or non-Newtonian flow (at ordinary temperatures and pressures) are unusual but not uncommon (e.g., "silly putty"). Materials whose viscosity decreases at high shear rates (e.g., paints that "thin out" as they are applied with a brush but then stiffen when quiescent) are examples of non-Newtonian fluids.

With respect to this experiment, a useful application of equation (1) to the case of mass transport through a circular tube of small internal diameter was derived by Poiseuille (1844):

$$\frac{dV}{dt} = \frac{\pi r^4 \Delta P}{8\eta L}, \quad (2)$$

where dV/dt is the volume flow rate of the liquid emerging from the tube, and r and L are, respectively, the radius and length of the tube. ΔP is the pressure difference across the ends of the tube and is the driving force for the bulk flow. Equation (2) assumes that the flow rate is slow and uniform. The viscosity coefficient, η , is called the *poise* in recognition of Poiseuille, and has cgs units. Thus one poise, P , is $1 \text{ g cm}^{-1} \text{ s}^{-1}$ (or dyne s). For many common liquids at room temperature, viscosities are about 0.002 to 0.04 P. For convenience, the centipoise (10^{-2} P), cP, is often used to report viscosity. In SI units, the viscosity coefficient is $\text{kg m}^{-1} \text{ s}^{-1}$ (or Pa s). $10^3 \text{ Pa s} = 1 \text{ cP}$.

Mixtures

From the way viscosity is defined, it follows that a mobile liquid is one that has a relatively low viscosity. Another useful parameter that applies to fluid mobility is *fluidity*, F , which is simply the reciprocal of the viscosity coefficient:

$$F = \frac{1}{\eta} . \quad (3)$$

One particular advantage to the use of fluidity is that the fluidities of mixed solutions of nonassociating liquids are often found (empirically) to be additive. Thus for a binary solution of liquids A and B , each pure liquid having fluidities F_A^\bullet and F_B^\bullet , respectively, the fluidity of a mixture containing mole fractions x_A and x_B may be approximated as

$$F \approx x_A F_A^\bullet + x_B F_B^\bullet , \quad (4)$$

i.e., a mole fraction-weighted linear combination of the pure liquid fluidities. The viscosity of the mixture is

$$F \approx \frac{1}{x_A/\eta_A^\bullet + x_B/\eta_B^\bullet} \quad (5)$$

and is obviously not linear in the composition variable, x_A (or x_B). Another approach for expressing the viscosity of a mixture is the following, proposed by Kendall (1913). For a binary solution,

$$\ln \eta = x_A \ln \eta_A^\bullet + x_B \ln \eta_B^\bullet \quad (6)$$

In this context, an *ideal solution* can be defined as one in which the interaction energies between the constituents are the same as those between the pure components. More specifically, it is assumed that in such a mixture the intermolecular interactions between identical molecules (e.g., $A-A$ and $B-B$) are equal to those between different molecules ($A-B$). The failure of component fluidities to be additive in the mixed state arises, then, either from the formation of association complexes between the components or from the destruction of such complexes that may be present in the pure component(s) after the pure components are mixed. Under these circumstances equations (5) and (6) would not be valid.

Temperature Dependence of Viscosity

It is found that over a reasonably wide temperature range, the viscosity of a pure liquid increases exponentially with the inverse absolute temperature. This relationship was first expressed

quantitatively by Arrhenius (1912):*

$$\eta = A \exp\left(\frac{E_\eta}{RT}\right), \quad (7)$$

where A is a constant for a given liquid, and E_η is sometimes called the activation energy to viscous flow of the liquid. Several theories have been proposed to rationalize equation (7). Simply viewed, however, an energy barrier must be surmounted in order for a molecule to "squeeze" by its neighbors if it is to undergo transport in the bulk medium. In so doing the transported molecule is overcoming intermolecular attractive forces. A plot of $\ln \eta$ vs. $1/T$ (sometimes called an Arrhenius plot) should, according to (7), be linear and have a slope equal to E_η/R .

Experimental Method The apparatus used in this experiment is called an Ostwald viscometer and is shown in Figure 2. Its design reflects the application of Poiseuille's law in that the liquid whose viscosity is being measured flows through a uniform capillary tube. In principle, the viscosity of a fluid could be measured absolutely using equation (2) if its flow rate was determined and the physical dimensions of the viscometer were known. However, it is more practical to calibrate a given viscometer with a liquid of known viscosity. The wisdom of this empirical approach can be appreciated by noting that, from Poiseuille's law, the viscosity depends on r^4 ; thus the error in measuring the capillary radius enters fourfold into the measured viscosity.

Operationally, the experiment consists of measuring the time required for a given volume of liquid to flow through the viscometer capillary. The driving pressure that forces the liquid through the capillary is provided by gravity; hence, the difference in driving force between the measured and calibrating liquids is accounted for through the respective densities of these liquids. The Ostwald viscometer is designed to keep the separation of the upper and lower levels of the flowing liquid as constant as possible. This is accomplished by the spherical bulbs on the feed and receive ends of the apparatus. The volume of liquid that flows through the viscometer is determined by the positions of two lines that are inscribed on either side of the feed bulb. These lines are called fiducial (fixed reference) marks. The experiment, then, consists of measuring the time required for the liquid meniscus to pass between the upper and lower fiducial marks of the viscometer.

We can readily integrate Poiseuille's law [equation (2)] and then express the viscosity as

$$\eta = \frac{\pi r^4 Pt}{8 VL}, \quad (8)$$

*Arrhenius is also associated with a similar equation that expresses the temperature dependence of a rate constant (see Experiment 21).

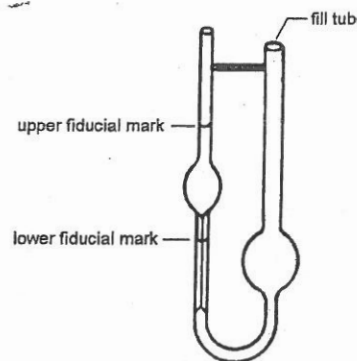


Figure 2. Ostwald viscometer.

where t is the elapsed time and V is the volume of liquid passing through the viscometer. The latter is constant for a given viscometer. Because the hydrostatic pressure, P , is proportional to the liquid density, ρ (the height is the same for both liquids), and the physical characteristics of the viscometer can be lumped into a constant, $k = r^4/8V$, the expression for viscosity becomes simply

$$\eta = kpt . \quad (9)$$

Thus if you measure the flow time, t , for a liquid having a density ρ you can determine its viscosity relative to that of some reference liquid, i.e.,

$$\eta = \frac{\eta_r \rho t}{\rho_r t_r} , \quad (10)$$

where η_r , ρ_r , and t_r are the viscosity, density, and flow time of the *reference* liquid, usually water. It is important that you carry out the set of measurements at a known and controlled temperature; hence, the η_r value pertains to this temperature.

Safety Precautions

- Safety goggles must be worn.
- This experiment requires the use of flammable materials. There should be no open flames in the laboratory. Fire extinguishers must be accessible at all times.
- **Methanol** and **toluene** are used in this experiment. These liquids must not come in contact with the skin. Gloves should be worn and eye protection MUST be used when handling these materials.
- The laboratory must be properly ventilated.

Procedure

Ostwald Viscometer

1. Suspend the viscometer in one of the constant-temperature baths using a clamp around a rubber sleeve attached to the viscometer. Make sure that the viscometer capillary is vertical and is below the surface of the water; see Figure 2. Adjust the temperature of the bath to 25.0°C by adding, if necessary, small amounts of crushed ice. Pipet 5 mL of distilled water into the viscometer. (Make all subsequent measurements using this volume of liquid and the same viscometer.) By placing the pipet bulb on the extended portion of the viscometer, and by gently squeezing the bulb, you should be able to push the liquid level up above the upper fiducial mark on the viscometer. Allow the water to run back down and start the electric timer exactly as the meniscus passes the upper fiducial mark. Stop the timer just as the meniscus passes the lower fiducial mark; record the elapsed time. Using the pipet bulb, bring the water back to the upper part of the viscometer and repeat the measurement. Do this until two or three measurements agree to within about 0.2 s.
2. Remove the viscometer from the bath. Clean and dry the viscometer by running a few milliliters of clean acetone through it using a pipet. Drain the acetone from the viscometer and carefully attach a suction tube from the aspirator to the viscometer. Aspirate for about a minute until the acetone has completely evaporated.
3. Prepare and label solutions of water and methanol that are 20, 40, 60, and 80% by volume methanol. Using the dried viscometer, determine the flow times of each of the methanol/water solutions at 25°C. Repeat each measurement until the flow times agree within about 0.2 s. After completing the measurement of one solution, rinse the viscometer with a few milliliters of the next solution to be studied. Complete the series by measuring the flow time for pure methanol.
4. Remove the viscometer from the bath. After draining the methanol, aspirate and reassemble the viscometer in the bath. Measure the flow times of a series of toluene/*p*-xylene solutions that are 0, 20, 40, 60, 80, and 100% by volume. Follow the procedure in step 3.
5. Remove the viscometer from the bath, clean it with acetone and aspirate. Suspend the viscometer in a water-filled 2-L beaker that is placed on a hot plate. Make sure the viscometer is fully immersed in the water. Add 5 mL of *p*-xylene and determine the flow time for a bath temperature of about 25°C. The exact temperature is not important as long as it is known to $\pm 0.5^\circ\text{C}$. Measure the flow times at higher temperatures, roughly every 10° up to about 65°C. Make sure that the temperature is constant and that the viscometer has had time to equilibrate to a new temperature. A 1000-W immersion heater can be used to accelerate the heating of the bath water; it must be disconnected well before the desired temperature is reached to avoid overshooting.

Data Analysis

1. Enter your run times for each set of experiments into a spreadsheet. Using equation (10) and the values of ρ , and η , transform these data into viscosities. Relevant data are presented in the appendix. Also transform the data to obtain the fluidity of each methanol/water and toluene/*p*-xylene mixture; compare these values with the fluidity calculated from equation (4).
2. Test the validity of equations (4) and (6) for the two binary systems studied.
3. Plot $\ln \eta$ vs. $1/T$ and determine the activation energy (and its standard deviation) for viscous flow for *p*-xylene.
4. Comment on the “ideality” of the two solutions.

Questions and Further Thoughts

1. Using a propagation-of-errors technique as applied to Poiseuille's law [equation (2)], show that the relative error in the capillary radius, ϵ/r , enters fourfold into the relative error of the viscosity.
2. Is it possible to have a homogeneous binary liquid solution whose viscosity is higher (or lower) than that of either of the two component liquids? What conclusions would you draw about the nature of intermolecular interactions in such a mixture?
3. In the case(s) in question 2, comment on the nature of the intermolecular forces of each pure liquid relative to the mixture.

Further Readings

- R. A. Alberty and R. J. Silbey, *Physical Chemistry*, 2d ed., pp. 710–713, Wiley (New York), 1997.
 P. W. Atkins, *Physical Chemistry*, 5th ed., pp. 833–834, W. H. Freeman (New York), 1994.
 I. N. Levine, *Physical Chemistry*, 4th ed., pp. 457–465, McGraw-Hill (New York), 1995.
 J. H. Noggle, *Physical Chemistry*, 3d ed., pp. 478–481, HarperCollins (New York), 1996.

Appendix

Table 1. Density of *p*-Xylene

T (°C)	D (g mL ⁻¹)	T (°C)	D (g mL ⁻¹)
20	0.879	45	0.839
25	0.857	50	0.834
30	0.852	55	0.830
35	0.848	60	0.825
40	0.943		

Table 2. Density of Methanol/Water Mixtures at 25°C

Methanol, volume %	Methanol, weight %	D (g mL^{-1})
0	0	0.977
20	16.54	0.971
40	34.57	0.944
40	54.33	0.909
80	76.02	0.859
100	100.	0.788

Table 3. Density of Toluene/*p*-Xylene Mixtures at 25°C

Toluene, volume %	D (g mL^{-1})
0	0.857
20	0.858
40	0.859
60	0.859
80	0.960
100	0.861

Experiment 17

Data Sheet A

Viscosity (Part I)

NAME _____

DATE _____

A chromatogram plot with 'Percent' on the y-axis and 'Time' on the x-axis. The y-axis has major tick marks at 0, 20, 40, 60, 80, and 100. There are four horizontal baseline lines. The first baseline is at 0%. The second baseline is at approximately 25%. The third baseline is at approximately 50%. The fourth baseline is at approximately 75%. The plot area shows a single sharp peak rising from the 0% baseline. The peak starts rising at approximately 10 minutes, reaches its maximum height at approximately 15 minutes, and then begins to decline back towards the baseline by 20 minutes.

Percent Toluene

Time

0

20

40

60

80

100

Temperature Time

Experiment 17

Data Sheet B

Viscosity (Part I)

NAME _____

DATE _____

Percent
Methanol

Time

Percent
Toluene

... Time

0	_____	_____	_____	_____
20	_____	_____	_____	_____
40	_____	_____	_____	_____
60	_____	_____	_____	_____
80	_____	_____	_____	_____
100	_____	_____	_____	_____

0	_____	_____	_____	_____
20	_____	_____	_____	_____
40	_____	_____	_____	_____
60	_____	_____	_____	_____
80	_____	_____	_____	_____
100	_____	_____	_____	_____

Temperature

Time

Experiment 32

Molecular Weight and Monomer Linkage Properties of Poly(vinyl alcohol)

Objective To determine the viscosity-average molecular weight of poly(vinyl alcohol) (PVOH) and the fraction of "head-to-head" monomer linkages in the polymer.

Introduction One of the fundamental molecular properties used to characterize a polymer is its molecular weight. Many of the physical characteristics of polymeric materials can be associated with the shape and weight distribution of the polymer. Some experimental techniques used to obtain this information are viscosity, osmotic pressure, and light scattering measurements. These measurements are made not on the polymer itself but on solutions containing the dissolved polymer. Because the viscosity and osmotic pressure of these solutions depend systematically on the concentration of polymer, they are called *colligative properties*.

This experiment deals with viscosity measurements of solutions of poly(vinyl alcohol) in water. This technique is very straightforward and does not require specialized equipment. We begin by reviewing the fundamentals of fluid viscosity. If a liquid undergoes laminar or streamline flow through a cylindrical tube, the differential equation that describes the mass transport in terms of the flow rate through a cylindrical tube is known as the Poiseuille law [named after Poiseuille (1844)], in whose honor the cgs unit of viscosity the poise ($1 \text{ g cm}^{-1} \text{ s}^{-1}$) is named. This equation is

$$\frac{dV}{dt} = \frac{\pi r^4 (P_0 - P')}{8\eta(z' - z_0)}, \quad (1)$$

in which dV is the volume of fluid (liquid or gas) transported in a time dt through a straight, cylindrical tube of radius r . The fluid is under a pressure difference $(P_0 - P')$ that extends over the length of the tube $(z_0 - z')$. If the pressure gradient is produced by the gravitational force acting on the fluid (the fluid flowing, for simplicity, in a downward vertical direction), $P_0 - P'$ is proportional to the density of the fluid, ρ . Hence for an arbitrary but constant volume of fluid, equation (1) yields (after integration)

$$V = \frac{t(\pi r^4 g \rho)}{8\eta}, \quad (2)$$

where g is the gravitational constant, and ρ is the bulk density of the fluid. We can rearrange equation (2) to give an expression for the fluid viscosity:

$$\eta = \frac{\pi r^4 g}{8V} \rho t = c \rho t \quad (\text{g cm}^{-1} \text{s}^{-1}), \quad (3)$$

where the constant c depends on the characteristics of the measuring device used, that is, the tube bore radius, r , and the total volume of fluid flowing in time t . Equation (3) is the basis for the measurement of liquid viscosities with an apparatus called a *viscometer*.¹ The constant c is determined by calibrating the viscometer with a liquid of a known viscosity, in this case water. The time t required for water to flow through the viscometer is measured. Knowledge of the water density (at the particular temperature) then allows c to be determined. For highly precise determinations of viscosity a kinetic-energy correction term must be subtracted from equation (3). Because this correction is usually less than 1% of the quantity $c \rho t$, it can be ignored.

We seek a relationship between the viscosity of a solution containing a dissolved high molecular weight polymer and some molecular weight property of the polymer itself. A significant contribution to this field was made by Einstein (1906), who showed that the *fractional change* in the viscosity of a solution—relative to the pure solvent—is related to the fraction of the total volume of solution occupied by the solute, in this case the polymer. It is assumed that the solute has simple spherical geometry. Thus the relevant equation is

$$\frac{\eta - \eta_0}{\eta_0} \equiv \eta_{sp} = \frac{Cv}{V}, \quad (4)$$

where η and η_0 are the respective viscosities of the solution and the pure solvent. The term η_{sp} [which is dimensionless and positive (because $\eta > \eta_0$)] is defined as the *specific viscosity* and is proportional to the ratio of the solute volume, v , to that of the solution, V . Thus η_{sp} is a *colligative property* because its value depends on the amount of polymer in solution, i.e., its concentration. The constant C has a theoretical value of 5/2 (for spherical solutes).

For a solution containing N spherical solute molecules each of radius R , equation (4) becomes (using $C = 5/2$ and $v = 4\pi R^3/3$)

$$\eta_{sp} = \frac{10\pi R^3 c_m}{3m}. \quad (5)$$

Equation (5) can more conveniently be expressed in terms of the mass concentration of the solute in the solution, c_m (defined as *grams per milliliter*), and the *molecular mass* of the solute, m , as (noting that $c_m = N_A m/V$)

$$\eta_{sp} = \frac{10\pi R^3 c_m}{3m}. \quad (6)$$

The colligative nature of η_{sp} is explicit in equation (6) because of the c_m dependence.

¹ See Experiment 17 for a description of the Ostwald viscometer.

Another quantity that will prove to be very useful is the *intrinsic viscosity*, $[\eta]$ (sometimes referred to as the Staudinger index):

$$[\eta] \equiv \lim_{c_m \rightarrow 0} \left(\frac{\eta_{sp}}{c_m} \right) = \frac{10\pi R^3}{3m} \quad (\text{cm}^3 \text{ g}^{-1}). \quad (7)$$

The limit of infinite dilution ($c_m \rightarrow 0$) is required to define a viscosity property that is intrinsic to the solute (in the given solvent), i.e., independent of the concentration. This approach essentially eliminates problems caused by the fact that the bulk properties of the polymer solution vary with concentration.

The limiting condition defined in equation (7) is needed to define $[\eta]$ because the reduced specific viscosity (i.e., η_{sp}/c_m) depends on the polymer concentration due to shear forces between the dissolved macromolecule and the solvent medium. This concentration dependence is observed to follow the relation

$$\frac{\eta_{sp}}{c_m} = [\eta] + k[\eta]^2 c_m + k' c_m^2, \quad (8)$$

where k , known as the Huggins constant, has a value of about 2 for rigid, uncharged spheres, and about 0.35 for flexible polymers in a "good" solvent.¹ The higher-order term in c_m in equation (8) can often be neglected. From equation (6) we can see that the ratio η_{sp}/c_m is not a colligative quantity; it is equal to an intrinsic property of the solute itself, namely, $10\pi R^3/3m$. The intrinsic viscosity has dimensions of $\text{cm}^3 \text{ g}^{-1}$ and is perhaps analogous to a molar volume. Because both η_{sp} and c_m are experimental quantities, equation (8) can be used to obtain $[\eta]$ by extrapolation to zero concentration.

It is interesting to note that if R is known, equation (7) can be used to determine m , the molecular mass of the solute, from $[\eta]$. Furthermore, the molecular weight of the solute divided by its mass provides Avogadro's number, which suggests an experimental approach for obtaining this fundamental constant. Conversely, if m is known, a value of the solute radius, R , can be determined from $[\eta]$. Following this reasoning, Einstein was able to obtain a satisfactory value of Avogadro's number as well as the molecular radii of carbohydrates. Few other direct experimental methods can be used to measure Avogadro's number.

Intrinsic viscosity measurements can be applied to a high molecular weight polymer to obtain its (spherical) radius, or its molecular weight. Remember that the value of R in equations (5) to (7) denotes the *effective* radius of the solute, because the solute may not be exactly spherical, and in addition, the solute may be associated with a (possibly large) number of solvent molecules. This effective radius is referred to as the *hydrodynamic radius* and can, in principle, vary for a given solute from solvent to solvent depending on what shape the solute adopts in a particular solvent, that is, the extent to which solvent molecules penetrate or stick to the solute.

Another complication that can be anticipated in applying equation (7) to molecules is that the assumption of spherical geometry may be invalid in some cases. Deviations from spherical geometry would manifest themselves theoretically in that C [in equation (4)] would have values

other than 5/2. In principle, this can be accounted for if the correct solvated molecular shape (oblate or prolate spheroid, oblong, etc.) is known.

A more serious problem encountered in dealing with high polymers is the fact that these systems consist of polymers of various chain lengths. Thus these are not homogeneous solutes (monodisperse) but have a distribution of molecular weights and are called *Polydisperse*. The degree to which a polymer is polydisperse depends on the conditions under which it is synthesized. Although in theory a polydisperse polymer can be fractionated into groups that have a more narrow molecular weight distribution (nearly monodisperse), this is often a long and tedious process. Measurements on raw, polydisperse polymer solutions provide information that is averaged over the molecular weights (and sizes) of the polymer. Such is the case in viscosity measurements.

In order to apply equation (7) to a system that is composed of a high molecular weight polydisperse polymer, a statistically averaged form of the molecular "radius" has to be used. In this experiment, the polymer studied—like many others—is a *linear* chain system, which means that the macromolecule is formed from a large number of monomer units in such a way that monomers add to the developing polymer chain without branching. Although the molecule is called a "linear" chain, its geometry surely does not resemble a straight-line assembly of monomer units. Rather, it is coiled up and adopts an overall shape that is approximately spherical. It may be thought to resemble a loosely tangled ball of yarn. See Figure 1.

This so-called random coil is not a static structure but continually undergoes contortionial motion as the different segments go through various conformational transitions. On a time-averaged basis, however, we can define a statistical radius called the *radius of gyration*, R_g . This characteristic property is expressed quantitatively as

$$R_g = \left(\frac{I}{m} \right)^{1/2}, \quad (9)$$

where m is the molecular mass and I is the moment of inertia, a second-order moment defined as

$$I = \sum_i m_i r_i^2, \quad (10)$$

in which the sum is over all the point masses, m_i (atoms), of the molecule, and r_i is the distance to the i th atom from the center of mass. We can calculate I only if we adopt some (static) structural model of the polymer. If we substitute the radius of gyration for the unique-valued radius R in equation (7), we have

$$[\eta] = \frac{N_A 10 \pi R_g^3}{3M} \quad (\text{cm}^3 \text{g}^{-1}), \quad (11)$$

where M , the molecular weight (along with N_A , Avogadro's number), replaces the molecular mass, m .

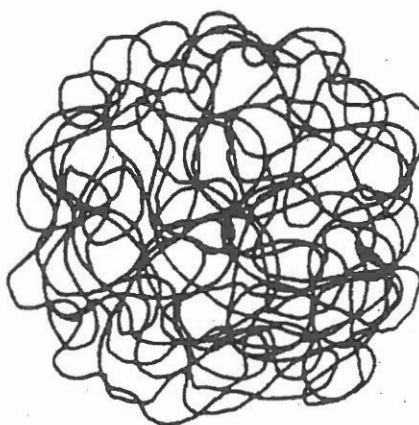


Figure 1. Schematic diagram of a linear chain polymer in a random-coil configuration.

If we now assume that the linear chain polymer is constructed of N monomer units linked together in such a way that *each* link is rotationally flexible, or unhindered (freely jointed chain), it can be demonstrated that the radius of gyration is proportional to the square root of the number of links in the polymer chain; thus $R_g \propto N^{1/2}$. This important conclusion is developed through the application of statistical mechanics to polymers.² Thus

$$[\eta] = K'M^{1/2}, \quad (12)$$

where K' is a proportionality constant that contains the conversion factor between R_g and $M^{1/2}$. Equation (12) is of particular importance in this experiment. It relates a measurable quantity, the intrinsic viscosity, to the desired molecular weight of the polymer. Although the square root dependence of $[\eta]$ on molecular weight is actually observed for some monodisperse polymer solutions, many others deviate from equation (12). The reasons for these discrepancies have to do with the nature of solvation and the effects brought about by solvent association on the structure of the polymer solute. Thus the molecules of a "good" solvent enter into the polymer coils to maximize solvolytic associations, and the polymer expands. Looked at another way, the polymer "swells" out into the solvent. In a "poor" solvent, on the other hand, the polymer knots up into itself and avoids the interactions with the solvent molecules. As you might expect, the solubility of a given polymer is larger in a good solvent than in a poor one. See Figure 2.

Another important consideration we have ignored thus far in the discussion is called the "excluded volume." This is the effective space that is inaccessible to a random coil or freely jointed chain. This volume cannot be occupied because the segments of the polymer avoid each other as they become too close during the twisting and turning that the polymer undergoes.

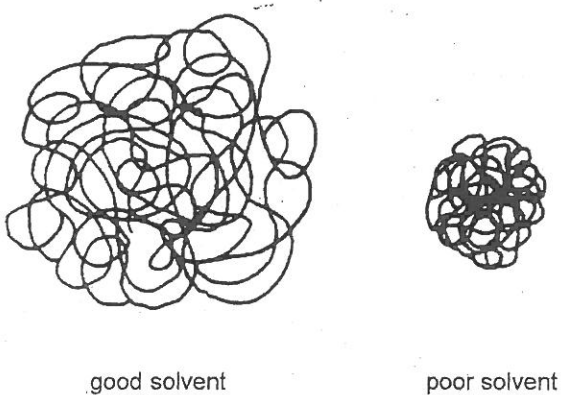


Figure 2. Schematic diagrams of a random-coil polymer in a "good" solvent (left) and a "poor" solvent (right).

A more general relationship between the intrinsic viscosity and molecular weight is provided by the Mark-Houwink equation:

$$[\eta] = KM^a \quad (\text{cm}^3 \text{ g}^{-1}), \quad (13)$$

where K and a are parameters that depend on the particular polymer, the solvent medium, and the temperature. Typically, a ranges between 0.5 and 0.8 [see equation (12)]. The Mark-Houwink parameters are obtained from log-log plots of $[\eta]$ vs. M for a series of monodisperse polymers. Agreement between K and a values obtained by different workers is often apparently poor.³ For example, for PVOH in water at 25°C, the following parameters shown in Table 1 have been reported.

Table 1. Mark-Houwink parameters for PVOH in water at 25°C.

K ($\text{cm}^3 \text{ g}^{-1}$)	a	Molecular Weight Range	Note*
0.020	0.76	$(0.6 - 2.1) \times 10^4$	4
0.30	0.50	$(0.9 - 17) \times 10^4$	5
0.14	0.60	$(1 - 7) \times 10^4$	6

* Notes appear at end of experiment.

We can obtain the molecular weight in explicit form from equation (13):

$$M_v = \left(\frac{1}{K} \right)^{1/a} [\eta]^{1/a} . \quad (14)$$

This expression (in which $[\eta]$ has dimensions of $\text{cm}^3 \text{ g}^{-1}$) is the computational basis of the experiment; it can be applied to polydisperse PVOH (which is used in this experiment), but the molecular weight obtained from equation (14) is a *viscosity-average* molecular weight, M_v . Statistically this quantity is different from the *number-average* molecular weight, M_n , which is obtained, for example, from osmotic pressure measurements. M_n is defined as

$$M_n = \sum_i f_i M_i , \quad (15)$$

where f_i is the fraction of polymers having molecular weight M_i ; the sum in equation (15) extends (in theory) from 0 to ∞ .

Flory and others⁷ have shown that the relationship between M_v and M_n is

$$\frac{M_v}{M_n} = [(1 + a)\Gamma(1 + a)]^{1/a} , \quad (16)$$

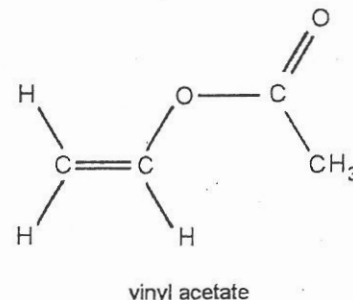
where a is the same parameter used in equation (13), and Γ denotes the *gamma function*, whose value (for a given a) can be obtained from mathematical tables. For example, for $a = 0.76$ (for PVOH in water at 25°C),⁴ the ratio in equation (16) is

$$\frac{M_v}{M_n} \equiv S = 1.89 . \quad (17)$$

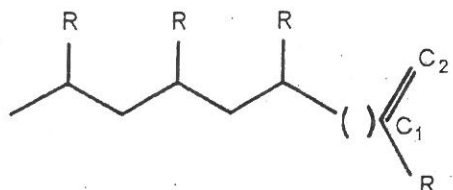
For $a = 0.50$ and 0.60 (see Table 1 on p. 498), S is 1.77 and 1.81, respectively.

Chemical Bonding in PVOH

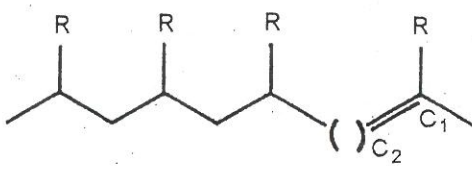
Poly(vinyl alcohol) is obtained from the hydrolysis of poly(vinyl acetate). The latter is synthesized from vinyl acetate monomers. Let us consider the question of how the vinyl acetate monomers link up to form the poly(vinyl acetate) polymer. The structure of vinyl acetate is shown.



It is an unsymmetrically substituted ethylene molecule, since only one end of the molecule is derivatized. Thus when a monomer is about to bond to the "growing" end of a polymer chain, it can do so in two ways with respect to the previously bonded monomer unit: Either the carbon atom containing the functional group, X, (C_1) can bond to the terminal end of the polymer chain or the unfunctionalized carbon (C_2) can form the bond. These alternatives are illustrated.



head-to-head

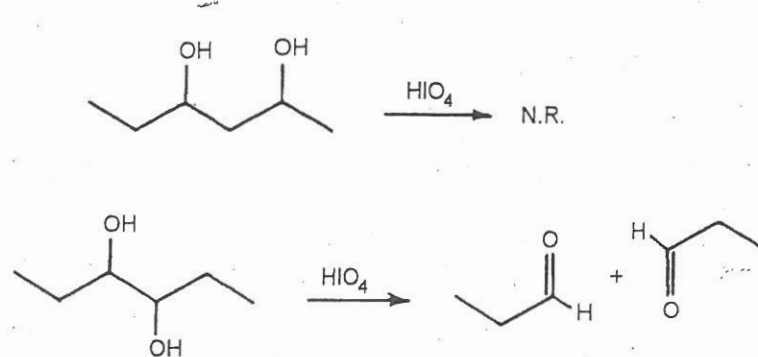


head-to-tail

An attachment in which the functional groups alternate is called "head-to-tail," and the one in which they are attached on adjacent carbon atoms is referred to as a "head-to-head" linkage. Because a head-to-head linkage involves considerable steric repulsion between the functional groups (they will have been added to *adjacent* carbon atoms on the polymer chain to form 1,2-substituents), it proceeds more slowly than a head-to-tail linkage. Therefore, a polymer will have a predominance of the latter arrangements, and the functional groups will, for the most part, alternate in their positions on the polymer backbone (i.e., repetitive 1,3-substituents).

Note also that if, after a head-to-head linkage has taken place, the next monomer attaches in a tail-to-tail fashion, the resulting arrangement between the substituents is a 1,4-disubstituted configuration. Considering the way this experiment is to be carried out (see the procedure), only the presence of head-to-head attachments is chemically significant. These result in the formation of 1,2-disubstituted structures on the polymer chain. The number of such events that occur in polymerization relative to the more common head-to-tail attachments (and thus 1,3-disubstituted structures) is of interest because the physical and chemical properties of the polymer depend on the fraction of such head-to-head linkages. Thus some analytical method for establishing this information is desirable.

In the case of the polymerization of vinyl acetate and the subsequent hydrolysis of the polymer to form PVOH, the consequence of a head-to-head linkage is the formation of a 1,2-diol (or vicinal glycol). The more common head-to-tail linkages result in the formation of 1,3-diols. The presence of 1,2-diol structures in the polymer can be conveniently distinguished from the 1,3-diols by a chemical means. The 1,2-diol is specifically cleaved (and oxidized) using periodic acid, HIO_4 . Actually, the reagent used is the periodate anion (from KIO_4), which hydrolyzes in water to form HIO_4 . The reaction is as follows:



Hence treatment of a PVOH sample with KIO_4 will split the polymer wherever a 1,2-diol structure exists. This results in a decrease in the (average) molecular weight of the polymer, and this change can be detected via viscosity measurements.

If we assume that the cleavage reaction is 100% effective (so that all the 1,2-diol linkages are cleaved), the increase in the number of solute molecules in the solution after treatment with KIO_4 divided by the total number of monomer units represented in the polymer sample is equal to the ratio of 1,2-diol structures to the total 1,2-diol *and* 1,3-diol arrangements in the system. This ratio, which is defined here as f , can be expressed as

$$f = \frac{\frac{1}{M_n'} - \frac{1}{M_n^0}}{\frac{1}{M^0}}, \quad (18)$$

where M_n^0 and M_n' are the number-average molecular weights of the polymer in the sample before and after the KIO_4 cleavage respectively. M^0 is the molecular weight of the monomer unit (CH_2CHOH), which is 44 u. Using the relationship between the number average and viscosity-average molecular weight for PVOH [see equation (17)], we get the following expression for the head-to-head fraction:

$$f = SM^0 \left\{ \frac{1}{M_v'} - \frac{1}{M_v^0} \right\}. \quad (19)$$

This equation provides the final result used in this experiment. It permits f to be determined from $[\eta]$ measurements of the PVOH sample before and after cleavage by KIO_4 . The value of S depends on the choice of α used in equation (16) (see Table 1).

Safety Precautions

- KIO_4 is an oxidant and should be handled cautiously.
- Always wear safety glasses in the laboratory.
- Make sure you have been shown how to use proper pipetting techniques. *Never* pipet by mouth.
- Handle the viscometer carefully to avoid breakage.

Procedure You will be provided with a clean viscometer. If the viscometer appears to be dirty, do not proceed with the experiment. Either obtain a clean one, or take the time to clean your viscometer thoroughly. Consult your instructor. If you do not remember how to use the viscometer, review the material in Experiment 16, or ask your instructor for this information. A stock solution of PVOH in water (c_m about 0.016 g mL^{-1}) should be available; if it is not, you will be told how to prepare this solution. This PVOH *must* have been appropriately filtered before use; undissolved particles will clog the viscometer. You will measure the viscosities of PVOH solutions of three or four different concentrations for both the cleaved and uncleaved polymers. You will calibrate the viscometer using pure water. Temperature control for each of these measurements is important.

1. Prepare 100 mL of a 50% solution of the PVOH stock solution. You will use this to prepare the diluted samples of the uncleaved polymer for measurement. Use purified (DI, RO, or distilled) water for the dilution in the volumetric flask. Cap and invert it several times gently. Do not agitate; this causes foaming. Because the polymer tends to adhere to the surface of glassware, rinse the pipet with water, then acetone, immediately after use. Aspirate dry. Follow this procedure whenever using glassware with PVOH solutions.
2. To prepare the *cleaved* polymer, pipet 50 mL of the stock solution into a 100-mL volumetric flask. Add 0.25 g of KIO_4 and about 20 mL of deionized water. Cap and swirl the liquid a few times. Place the mixture in a hot-water bath ($\sim 70^\circ\text{C}$) for several minutes until the solid dissolves; periodically mix the solution if necessary. After the solid has dissolved, remove the flask and let it cool to room temperature, then fill to the mark with deionized water. Gently invert it several times. Label the flask.
3. There are now two PVOH solutions (one cleaved and one uncleaved), each with c_m of about 0.0080 g/mL. From each of these prepare 50 mL of solutions corresponding to 80, 60, and 40% of that concentration. Make up the 40% solution from the 80% one. Label these new samples *immediately* after preparation. Place them all in a 25°C bath.
4. Calibrate the viscometer with purified water. Pipet 5 mL of water into the viscometer, which is clamped and held in a 25°C bath. Using a pipet bulb, carefully “push” the water up through the capillary tube until it is above the upper fiducial mark. Remove the bulb and allow the water to drain. Start the timer or stopwatch exactly as the water meniscus passes the upper fiducial mark; stop the timer just as the meniscus passes the lower mark. Record this time. Repeat this measurement at *least* three times. Use the pipet bulb to “reset” the liquid. Alternatively, use a

flexible tube connected to an aspirator. The timings should be within 0.2 to 0.5 s. After the calibration is complete, remove the viscometer from the bath.

- Following the same procedure, measure the viscosities of the cleaved and uncleaved samples, starting with the most dilute samples. Make each measurement in triplicate.

Calculations and Data Analysis

- Calibrate the viscometer. Determine the constant c in equation (3) from the mean flow time of water and its density and viscosity at 25°C.
- Determine and tabulate the viscosities and specific viscosities of the PVOH samples. Assume they have densities equal to that of pure water. In the same table list the bulk c_m values (g mL^{-1}) of the PVOH samples.
- For each sample determine $[\eta]$ for the uncleaved and cleaved polymer. Also determine the Huggins constant. See equation (8).
- Choose a set of K and α values, and using the appropriate relations, determine values of M_v for the uncleaved and cleaved PVOH, as well as the head-to-head ratio, f . Comment on the magnitudes of your results.
- Determine M_v and f for another set of K and α values and compare them with the results in step 4.

Questions and Further Thoughts

- Consult a table of mathematical functions, and using the appropriate gamma functions and equation (16), verify the values of S cited in and after equation (17).
- Using the definition of f [see the discussion before equation (18)], derive equation (18) and use the result in (17) to obtain equation (19).
- Viscosity measurements are often performed on proteins and other biopolymers. What experiments could be carried out on such molecules to examine the effect of solution conditions (e.g., ionic strength, or pH) on the extent of denaturation (breakdown of the biologically active structure)?
- Specific and intrinsic viscosities provide structural information about macromolecules under the assumption that the solute is spherical [see equation (4)]. Is this a good assumption for a polymer such as PVOH? For what sort of macromolecule would you expect this assumption to be poor?
- How would the structure of a polymer such as PVOH in the vapor phase differ from that in aqueous solution?
- The intrinsic viscosity of a sample of polydisperse PVOH in water was determined to be $86 \text{ cm}^3 \text{ g}^{-1}$ at 298 K. Using the information in Table 1 and the Mark-Houwink equation, what range of molecular weights can be reported for the polymer?

Notes

1. C. Tanford, *Physical Chemistry of Macromolecules*, pp. 390-392, Wiley (New York), 1961.
2. Ibid. pp. 138-168.
3. See J. Bandrup and E. H. Immergut, eds., *Polymer Handbook*, vol. 2, IV-14, Wiley (New York), 1975.
4. P. J. Flory and F. S. Leutner, *J. Poly. Sci.*, 3:880 (1948); 5:267 (1950).
5. K. Dialer, K. Vogler, and F. Patat, *Helv. Chim. Acta*, 35:869 (1952).
6. H. A. Dieu, *J. Poly. Sci.*, 12:417 (1955).
7. J. R. Schaeffgen and P. J. Flory, *J. Am. Chem. Soc.*, 70:2709 (1948).

Further Readings

- R. A. Alberti and R. J. Silbey, *Physical Chemistry*, 2d ed. pp. 769-771, Wiley (New York), 1997.
P. W. Atkins, *Physical Chemistry*, 5th ed., pp. 798-799, W. H. Freeman (New York), 1994.
I. N. Levine, *Physical Chemistry*, 4th ed., pp. 464-465, McGraw-Hill (New York), 1995.
J. H. Noggle, *Physical Chemistry*, 3d ed., pp. 486-488, HarperCollins (New York), 1996.
J. F. Swindells, R. Ullman, and H. Mark, Determination of Viscosity, vol. 1, p. 1, chap. XII of *Techniques of Organic Chemistry*, 3d ed., A. Weissberger, ed. Interscience (New York), 1959.

Experiment 32

Data Sheet A

Intrinsic Viscosity

NAME _____

DATE _____

I. Viscometer calibration: Bath temperature _____

Stock solution concentration _____

Flow times, s _____

II. Cleaved samples: Bath temperature _____

Flow Times, s

Sample 1	Sample 2	Sample 3
_____	_____	_____
_____	_____	_____
_____	_____	_____
_____	_____	_____
_____	_____	_____

III. Uncleaved samples: Bath temperature _____

Flow Times, s

Sample 1	Sample 2	Sample 3
_____	_____	_____
_____	_____	_____
_____	_____	_____
_____	_____	_____
_____	_____	_____

Experiment 32

Data Sheet B

Intrinsic Viscosity

NAME _____

DATE _____

II. Viscometer calibration: Bath temperature _____

Stock solution concentration: _____

Flow times, s: _____

II. Cleaved samples: Bath temperature _____

Flow times, s

Sample 1

Sample 2

Sample 3

III. Uncleaved samples: Bath temperature _____

Flow Times, s

Sample 1

Sample 2

Sample 3

FOR STUDENTS

Emission Spectroscopy: Biophysics and FRET

- Goals:**
- (1) Determine the free energy associated with unfolding a protein
 - (2) Understand principles of quenching via Förster energy transfer
 - (3) Calculate intramolecular distances for partially unfolded and fully folded structures

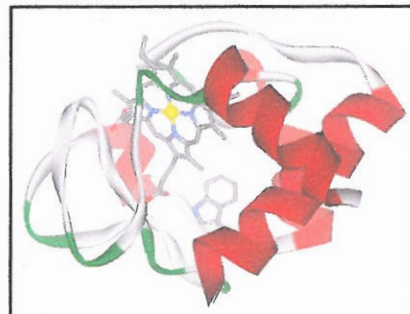
Resources: Handouts from Lakowicz (chapter 13) (1), Jones (2), and Pace (3).

Introduction and Background

The study of biological macromolecular structure has become a major field in biochemistry and chemistry research laboratories. Different spectroscopic techniques, such as UV-Vis absorption, fluorescence, and circular dichroism, have been employed to investigate the thermodynamics and structural changes associated with protein folding and unfolding. In undergraduate laboratories, most experiments rely on one technique to study a chemical problem. Here, we describe a multifaceted approach towards the study of the important biophysical problem of protein folding. Specifically, the combination of absorption, fluorescence, and Förster resonance energy transfer (FRET) techniques will provide complementary and indepth information on structural changes and thermodynamics associated with these changes. The protein used in this experiment is a well-studied system, cytochrome *c* (cyt *c*). Cyt *c* will be unfolded chemically via a denaturant and monitored spectroscopically.

FRET is a spectroscopic technique that may be used to determine inter- or intramolecular distances. It has been applied to study a wide variety of systems to obtain structural information. FRET occurs via long-range dipole-dipole interactions between donor and acceptor molecules, and does not involve emission of a photon. Radiationless energy transfer from an excited-state donor to a ground-state acceptor is the fundamental principle behind FRET. A critical requirement for FRET is spectral overlap between the emission spectrum of the donor and the absorption spectrum of the acceptor. The efficiency of FRET energy transfer is inversely proportional to the sixth power of the distance between the donor and acceptor. By utilizing this distance dependence, structural information about proteins can be obtained during denaturant-induced unfolding.

Cytochrome *c* is an electron transfer protein found in the inner membrane of mitochondria. This globular protein consists of a single polypeptide chain that contains one tryptophan residue at position 59 (Trp-59) and a covalently bound heme cofactor. The intrinsic fluorophore, tryptophan, serves as the FRET donor while the heme cofactor serves as the acceptor. In the native structure of cytochrome *c*, Trp-59 is in close proximity to the heme group (shown on the right). When the protein is folded, energy is transferred from the excited tryptophan to the heme group, causing the tryptophan fluorescence to be quenched. Upon addition of a chemical denaturant to unfold the protein, the rise in fluorescence signal from Trp-59 indicates that the distance between donor and acceptor has increased; this change in distance as a function of folding state can be quantified via the equations that describe FRET.



FRET Theory

According to Förster's theory on energy transfer, the rate of energy transfer k_T is related to the lifetime of the donor in the absence of acceptor (τ_D) and the distance between the donor and acceptor (r) via

$$k_T(r) = \frac{1}{\tau_D} \left(\frac{R_0}{r} \right)^6 \quad (1)$$

The Förster distance, R_0 , is the critical distance for energy transfer, and is defined as the distance at which the efficiency of energy transfer is 50%. Förster distances typically range from 20-60 Å, and can be calculated using the relationship

$$R_0^6 = 8.79 \times 10^{23} [\kappa^2 n^{-4} \Phi_D J_{DA}(\lambda)] \quad \text{in } \text{\AA}^6 \quad (2)$$

where κ^2 is the orientation factor between the transition dipoles of the donor and acceptor, n is the refractive index of the solvent, Φ_D is the quantum yield of the donor in the absence of acceptor, and J_{DA} is the overlap integral of the donor emission spectrum and the acceptor absorption spectrum. The overlap integral can be calculated as follows:

$$J_{DA}(\lambda) = \frac{\int F_D(\lambda) \varepsilon_A(\lambda) \lambda^4 d\lambda}{\int F_D(\lambda) d\lambda} \quad (3)$$

J_{DA} is in M^{-1}cm^3 , $F_D(\lambda)$ is the fluorescence of the donor in absence of acceptor, and $\varepsilon_A(\lambda)$ is the extinction coefficient of the acceptor at λ . FRET energy transfer efficiency, E , is defined by the following relationship:

$$E = \frac{R_0^6}{R_0^6 + r^6} \quad (4)$$

Efficiency can be experimentally determined using the fluorescence intensities of the donor with and without the acceptor in the form of Equation 5:

$$E = 1 - \frac{F_{DA}}{F_D} \quad (5)$$

where F_{DA} is the fluorescence intensity of the donor in the presence of the acceptor, and F_D is the fluorescence intensity of the donor in the absence of the acceptor.

Free energy of Protein Unfolding

Native tertiary structures of biomolecules can be disrupted by a variety of methods, including changes in temperature and pH, as well as addition of chemical denaturants. Two common chemical denaturants, guanidinium hydrochloride and urea, are used to disrupt native protein structures easily. The mechanisms by which these denaturants unfold proteins is an active area of research, and hypotheses regarding their modes of action involve direct solvation of peptide bonds and other hydrophobic regions as well as significant modification of solvent structures. By measuring the relative concentrations of folded and unfolded proteins as a function of denaturant concentration, one generates an unfolding curve which can be further analyzed to determine protein stability.

Spectroscopic techniques are commonly used to determine relative concentrations of folded and unfolded proteins for a given denaturant concentration. A critical requirement is that the folded and unfolded species exhibit unique spectroscopic signatures. Typical optical methods that may distinguish between native and denatured structures include circular dichroism, UV-Vis absorption spectroscopy, and fluorescence spectroscopy. Shifts in absorption/emission maxima as well as changes in intensities often reflect changes in global and local protein structures. By utilizing these spectroscopic shifts to monitor changes in population, unfolding curves can be generated to yield free energies of unfolding in the absence of denaturant.

The simplest model of protein folding/unfolding describes a two-state system of folded (F) and unfolded (U) species:



The equilibrium constant and free energy of unfolding are then given as

$$K_{eq} = \frac{[U]}{[F]} \quad \text{and} \quad \Delta G_U^o = -RT \ln K_{eq} = -RT \ln \frac{[U]}{[F]} \quad (7) \text{ and } (8)$$

where ΔG_U^o is the free energy of unfolding in denaturant. Here, we are interested in the free energy of unfolding in the absence of denaturant. A theoretical treatment described by Pace (1984) and Jones (1997) approximates a linear perturbation of free energy as a function of denaturant concentration wherein extrapolation of this relationship to zero denaturant concentration gives rise to the free energy of unfolding in the absence of denaturant, $\Delta G_{H_2O}^o$:

$$\Delta G_U^o = \Delta G_{H_2O}^o - mC \quad (9)$$

Here, m ($\text{kcal M}^{-1} \text{ mol}^{-1}$) describes the rate of change of the free energy of denaturant with respect to denaturant concentration and C (M) is the molar concentration of denaturant.

The denaturant concentration that gives rise to equal populations of folded and unfolded proteins is referred to as the midpoint concentration, C_m . At C_m , the free energy of unfolding is zero so that

$$\Delta G_{H_2O}^o = mC_m \quad (10)$$

Using the definition of fraction of unfolded molecules, f , given by:

$$f = \frac{[U]}{[U] + [F]} \quad (11)$$

it is relatively straightforward to obtain the following equation:

$$f = \frac{\exp\left[-m\left(\frac{C_m - C}{RT}\right)\right]}{1 + \exp\left[-m\left(\frac{C_m - C}{RT}\right)\right]} \quad (12)$$

Experimental data points in an unfolding curve are fit to Equation 12, with f and C as dependent and independent variables, respectively, to yield values for m and C_m . Knowledge of the variables m and C_m then allows for determination of the free energy of unfolding in the absence of denaturant, $\Delta G_{H_2O}^o$, using Equation 10.

Lab procedure

In this experiment, you will determine the free energy of unfolding ferric cyt c using the chemical denaturant urea. You will monitor changes in fluorescence from Trp-59 as a function of urea concentration to generate an unfolding curve for cyt c (part A). In part B, you will determine the Förster distance of the trp-heme pair using a tryptophan model compound, n-acetyl-trypophanamide, to approximate the donor in absence of acceptor (F_D). The cyt c absorption spectrum is used to determine $\varepsilon_A(\lambda)$ of the acceptor. Finally, in part C, you will combine the knowledge gained in parts A and B to determine changes in distance between Trp-59 and the heme moiety as a function of denaturant.

Instruments: Follow lab manual instructions for the fluorometer and absorption spectrometer.

A. Measurement of unfolding curve

1. Turn on the instrument immediately upon arriving in the laboratory.
2. Prepare a stock solution (50 mL) of 20 mM pH 7.4 phosphate buffer. This buffer is called KP_i. Both components of the conjugate acid-base pair should be weighed out separately to obtain the desired ratio and then dissolved in water. Use potassium phosphate monobasic (CAS 7778-77-0) and potassium phosphate dibasic (CAS 7758-11-4).
3. Prepare a stock solution (50 mL) of 10.0 M urea (CAS 57-13-6) in KP_i. You should add the urea and phosphates to an empty graduated cylinder and add water up to 50 mL. This solution is called urea/KP_i.

4. Prepare a stock solution (0.8 mL of about 500 μM) of cyt *c* (CAS 9007-43-6) in KP_i (ϵ_{410} for cyt *c* in this solution is approximately 105,000 $\text{M}^{-1}\text{cm}^{-1}$, ϵ_{530} is 11,200 $\text{M}^{-1}\text{cm}^{-1}$).
5. Prepare several $\sim 10 \mu\text{M}$ cyt *c* (1.5 mL each) samples by mixing the appropriate amounts of stock solution made in part A4 with stock solutions made in parts A3 and A2 to achieve final urea concentrations of 0.0 to 10.0 M in 0.5 M increments. You should have 21 samples in 21 plastic Eppendorf tubes.
6. Record fluorescence and absorption spectra of KP_i, urea/KP_i, and each of the 21 samples prepared in part A5. The fluorescence spectra should be recorded with 290 nm excitation, and scanned from 305 nm to 500 nm. Use “high” sensitivity and 5 nm bandpass for both excitation and emission. These spectra will be used to determine the free energy of unfolding of cyt *c* using fluorescence changes of Trp-59 as the probe. You will see a large peak at ~ 323 nm in spectra of the buffers KP_i and urea/KP_i as well as in some of your cyt *c* samples. Talk to the Professor or TAs to understand the origin of this peak.
7. To obtain an unfolding curve, subtract background fluorescence spectra of the buffers KP_i or urea/KP_i from corresponding fluorescence spectra of protein to obtain a corrected fluorescence spectrum. These corrected fluorescence spectra should be made using the general procedure:

Spectrum A = raw fluorescence from cytochrome *c* in buffer/denaturant

Spectrum B = raw fluorescence from buffer/denaturant

Corrected Spectrum = Spectrum A - B

The fluorescence intensity of the corrected spectrum at 350 nm should then be normalized for protein concentration (via the absorption value at 530 nm), and plotted as a function of urea concentration. The y-axis should be scaled from 0 to 1 (max). What is the free energy of unfolding? You will need Equations 10 and 12. Fitting your data to Equation 12 is best accomplished with advanced analytical software, such as Matlab or Igor Pro. You may also use the “Solver” tool in Excel.

8. If time permits, note the change in absorption spectra as a function of unfolding. Plot the shift in Soret absorption near 410 nm as a function of denaturant concentration to generate an unfolding curve and determine the free energy of unfolding for cyt *c*. How do these results differ from part A7 and what are possible origins of the differences (if any)?

B. Determination of the Förster distance

1. Prepare 5 mL of a $\sim 10 \mu\text{M}$ solution of the tryptophan model compound, N-acetyltryptophanamide (NATA) (CAS 2382-79-8) in KP_i. The actual concentration is not important, as long as you are not saturating the fluorometer detector. You may need to start with a concentrated stock solution of NATA and dilute it to the desired $\sim 10 \mu\text{M}$. Regardless of how you prepare the sample, you must determine the actual concentration based on the value for the extinction coefficient at 280 nm (ϵ_{280} for NATA is 5630 $\text{M}^{-1}\text{cm}^{-1}$).
2. Measure absorption and fluorescence spectra of the solution prepared in part B1.

3. Use the fluorescence spectrum collected in part B2 along with the absorption spectrum of ~10 μM cyt *c* (0.0 M urea) from part A6 to calculate the Förster distance of the trp-heme pair. You will need Equations 2 and 3. Determination of the integrated areas can be done numerically by approximating the integral as a sum, or with advanced software such as Matlab or Igor Pro. Other pertinent information: $\kappa^2=2/3$, $n=1.4$, $\Phi_D=0.13$.

C. Calculation of intramolecular distances for unfolded structures

1. Using Equation 4 and your calculated R_0 from part B3, make a graph of energy transfer efficiency (E) as a function of distance, r , between donor and acceptor. This is the theoretical distance dependence of energy transfer for your donor-acceptor pair.
2. Use Equations 4 and 5 and the corrected and normalized (for concentration) spectra from part A6 to determine the distance between Trp-59 and the heme group as a function of denaturant concentration. For F_D , you should use the fluorescence intensity of NATA at the same concentration as the cyt *c* samples. Compare the distance between Trp-59 and the heme group for the fully folded protein (0.0 M urea) with distances obtained from the known crystal structure (PDB 1HRC). How do these compare?
3. What assumptions are made to determine $\Delta G_{H_2O}^o$ from part A and intramolecular distances from part C? Do these assumptions conflict?

D. Optional

1. Generate an unfolding curve using 0.0 to 6.0 M guanidinium chloride (gdmHCl) (CAS 50-01-1) instead of urea as the denaturant. Because the pK_a of phosphate buffer is sensitive to ionic strength, you must adjust the pH of each cyt *c* + gdmHCl solution to 7.4 prior to making fluorescence and absorption measurements. How does the measured conformational stability of cyt *c*, $\Delta G_{H_2O}^o$, differ when measured with this other denaturant? What intermolecular forces may impact this difference in thermodynamic stability?
2. Index of refraction may be used for accurate determination of denaturant concentration (4). What are the principles of index of refraction?

Hazards: Urea is a skin irritant; guanidinium hydrochloride is a skin, eye, and respiratory tract irritant. If denaturant comes in contact with any of the above areas, wash with copious amounts of water. General laboratory safety practices should be followed. Gloves, safety glasses, and lab coat should be worn at all times. Care should be taken while handling proteins. While cytochrome *c* and phosphate buffer are relatively harmless, other proteins and buffers can be potentially hazardous.

E. References

- (1) Lakowicz, J. R. *Principles of Fluorescence Spectroscopy*, 3rd ed.; Springer: New York, 2006.
- (2) Jones, C. M. *J. Chem. Educ.* **1997**, *74*, 1306-1310.
- (3) Pace, C. N. *Methods Enzymol.* **1986**, *131*, 266-280.
- (4) Shirley, B. A. Urea and guanidine hydrochloride denaturation curves. In *Protein Stability and Folding*; Shirley, B. A., Ed.; Human Press Inc.: Totowa, 1995; Vol. 40; pp 177-190.

J. A. Weil, J. R. Bolton, and J. E. Wertz, *op. cit.*

A useful compilation of EPR data is J. A. Pedersen, *Handbook of EPR Spectra from Quinones and Quinols*, CRC Press, Boca Raton, Fla. (1985).

EXPERIMENT 42

NMR Determination of Keto-Enol Equilibrium Constants

In this experiment, proton NMR spectroscopy is used in evaluating the equilibrium composition of various keto-enol mixtures. Chemical shifts and spin-spin splitting patterns are employed to assign the spectral features to specific protons, and the integrated intensities are used to yield a quantitative measure of the relative amounts of the keto and enol forms. Solvent effects on the chemical shifts and on the equilibrium constant are investigated for one or more β -diketones and β -ketoesters.

THEORY

Chemical Shifts. In Exp. 33, the Zeeman energy levels of a nucleus in an external applied field were given as

$$E_N = -g_N\mu_N M_I B_{\text{loc}} \quad (1)$$

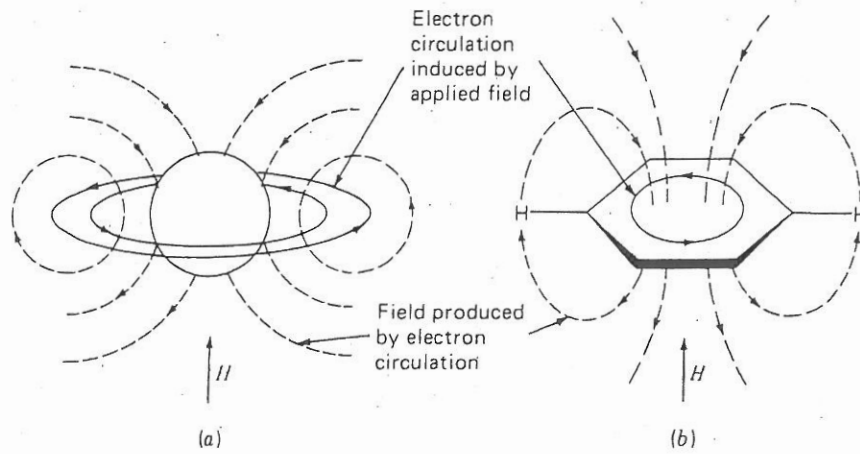
where B_{loc} is the magnetic induction ("local field") at the nucleus. As a result of the $\Delta M_I = \pm 1$ selection rule, a transition will occur at frequency

$$\nu_i = \left(\frac{g_N\mu_N}{h} \right) B_{i,\text{loc}} \quad (2)$$

for a nucleus i . The chemical shift in parts per million (ppm) of this nucleus relative to a reference nucleus r is defined by

$$\delta_i \equiv \frac{\nu_i - \nu_r}{\nu_r} \times 10^6 \approx \frac{B_r - B_i}{B_r} \times 10^6 \quad (3)$$

Here the first definition is based on the resonant frequencies for a fixed external induction (field) B , whereas the second (nearly equivalent) relation is based on the more common experimental case where B is varied to achieve resonance at a fixed instrumental frequency ν . Tetramethylsilane (TMS) is usually used as the proton reference, since it is chemically inert and its 12 equivalent protons give a single transition at a field B_r , higher than the field B_i found in most organic compounds. Thus δ is generally positive and increases when substituents are added that attract electrons and thereby reduce the shielding about the proton. This shielding arises because the electrons near the proton are induced to circulate by the applied field B (see Fig. 1a). This electron current produces a secondary field that opposes the external field and thus reduces the local field at the proton. As a result, resonance at a fixed frequency such as 60 MHz requires a higher external field for protons with larger shielding. This shielding effect is generally restricted to electrons localized on the nucleus of interest, since random tumbling of the molecules causes the effect of secondary fields due to electrons associated with neighboring nuclei to average to zero. Nuclei such as ^{19}F , ^{13}C , and ^{11}B have more local electrons than hydrogen, hence their chemical shifts are much larger.

**FIGURE 1**

Shielding and deshielding of protons: (a) shielding of proton due to induced diamagnetic electron circulation; (b) Deshielding of protons in benzene due to aromatic ring currents.

Long-range *deshielding* can occur in aromatic and other molecules with delocalized π electrons. For example, when the plane of the benzene molecule is oriented perpendicular to B , circulation of the π electrons produces a ring current (see Fig. 1b). This ring current induces a secondary field at the protons that is *aligned parallel* to B and thus increases the local field at the protons. This induced field changes with benzene orientation but does not average to zero, since it is not spherically symmetric. Because of this net deshielding effect, the resonance of the benzene protons occurs at a relatively low external field. The proton chemical shift δ for benzene is 7.27, greatly downfield from the value $\delta = 1.43$ that is observed for cyclohexane, in which ring currents do not occur. Similar deshielding occurs for olefinic and aldehydic protons because of the π electron movement. Typical values of δ for different functional groups are shown in Table 1, and additional values are available in Refs. 1 to 3. Although the resonances change somewhat for different compounds, the range for a given functional group is usually small and δ values are widely used for structural characterization in organic chemistry.

TABLE 1 Typical proton chemical shifts δ

		Acetylenic protons	
CH ₃ protons			
(CH ₃) ₄ Si	0.0	HOCH ₂ C≡CH	2.33
(CH ₃) ₄ C	0.92	CICH ₂ C≡CH	2.40
CH ₃ CH ₂ OH	1.17	CH ₃ COC≡CH	3.17
CH ₃ COCH ₃	2.07	Olefinic protons	
CH ₃ OH	3.38	(CH ₃) ₂ C=CH ₂	4.6
CH ₃ F	4.30	Cyclohexane	5.57
CH ₂ protons		CH ₃ CH=CHCHO	6.05
Cyclopropane	0.22	Cl ₂ C=CHCl	6.45
CH ₃ (CH ₂) ₄ CH ₃	1.25	Aromatic protons	
(CH ₃ CH ₂) ₂ CO	2.39	Benzene	7.27
CH ₃ COCH ₂ COOCH ₃	3.48	C ₆ H ₅ CN	7.54
CH ₃ CH ₂ OH	3.59	Naphthalene	7.73
CH protons		α -Pyridine	8.50
Bicyclo[2.2.1]heptane	2.19	Aldehydic protons	
Chlorocyclopropane	2.95	CH ₃ OCHO	8.03
(CH ₃) ₂ CHOH	3.95	CH ₃ CHO	9.72
(CH ₃) ₂ CHBr	4.17	C ₆ H ₅ CHO	9.96

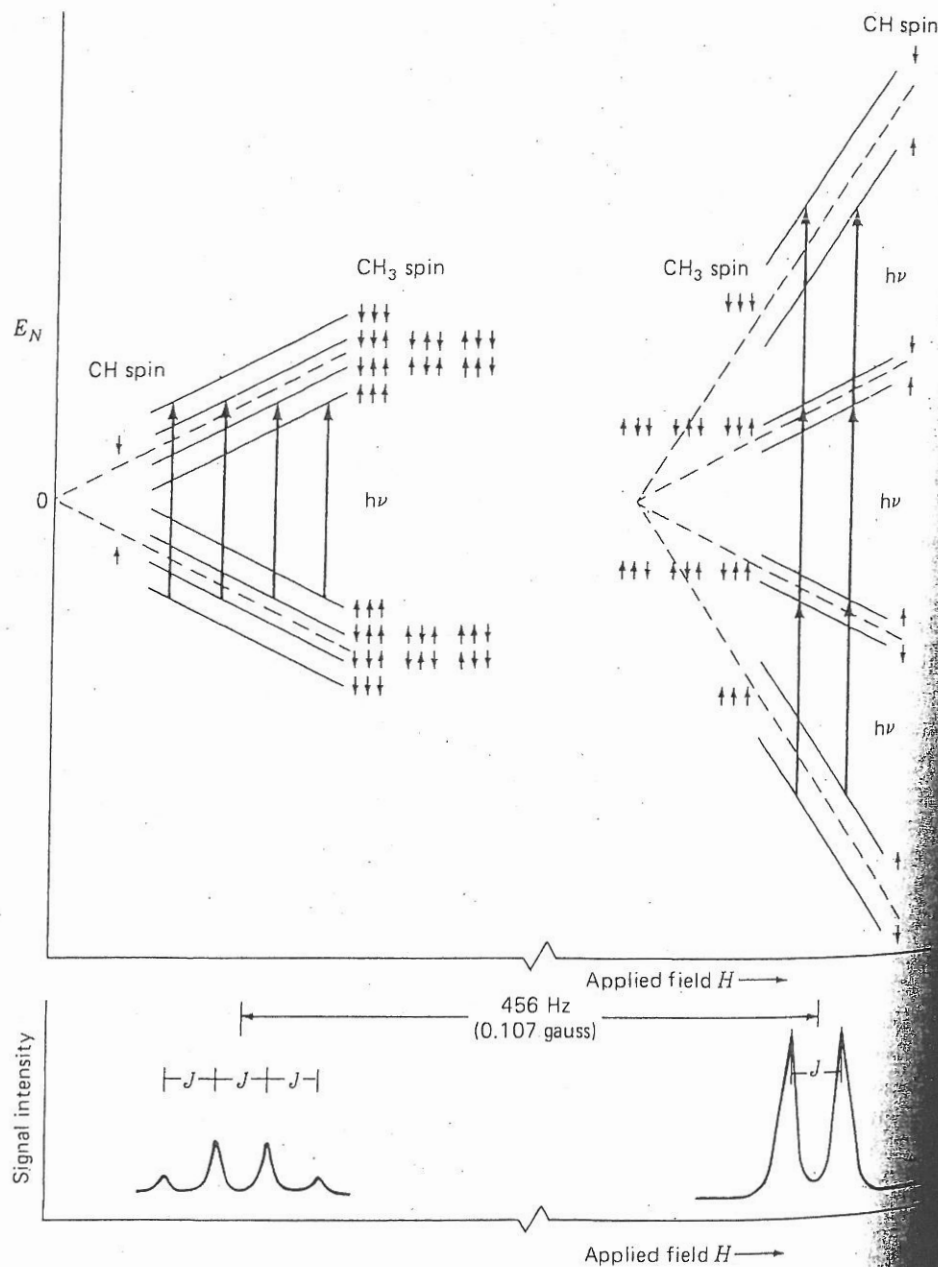
Spin-Spin Splitting. High-resolution NMR spectra of most organic compounds reveal more complicated spectra than those predicted by Eq. (2), with transitions often appearing as multiplets. Such *spin-spin splitting patterns* arise because the magnetic moment of one proton (A) can interact with that of a nearby nucleus (B), causing a small energy shift up or down depending on the relative orientations of the two moments. The energy levels of nucleus A then have the form

$$E_A = -g_{N_A}\mu_N M_{I_A}(1 - \sigma_A)B + hJ_{AB}M_{I_A}M_{I_B} \quad (4)$$

and there is a similar expression for E_B . The spin-spin interaction is characterized by the coupling constant J_{AB} , and the effect is to split the energy levels in the manner illustrated for acetaldehyde in Fig. 2. It is apparent from this diagram that the external field B does

FIGURE 2

Energy levels, transitions, and 60-MHz NMR spectrum for acetaldehyde (CH_3CHO). The coupling constant $J = J_{\text{CH}_3} = J_{\text{CH}} = 2.2 \text{ Hz}$ ($= 5.2 \times 10^{-4} \text{ gauss} = 5.2 \times 10^{-8} \text{ T}$). For CH, the quantum number $M_I = -\frac{1}{2}$ or $\frac{1}{2}$. For the CH_3 group, $M_I = -\frac{3}{2}, -\frac{1}{2}, +\frac{1}{2}, +\frac{3}{2}$. The dashed lines represent the level spacing that would occur in the absence of the spin-spin interaction. The slopes of the energy levels are greatly exaggerated in the figure. Also, to be correct, all dashed lines should extrapolate to a common $E_N = 0$ at $H = 0$.



not effect the small spin-spin splitting that is characterized by the coupling constant J . The quantity J is a measure of the strength of the pairwise interaction of the proton spin with the spin of another nucleus. Since there are only proton-proton interactions in acetaldehyde, the same splitting occurs for both CH and CH_3 resonances.

The total integrated intensity of the CH and CH_3 multiplets follows the proton ratio of 1:3. However, the intensity distribution within each multiplet is determined by the relative population of the lower level in each transition. Since the level spacing is much less than kT , the Boltzmann population factors are essentially identical for these levels. However, there is some degeneracy because rapid rotation of the CH_3 group around the C-C bond makes the three protons magnetically equivalent. The number of spin orientations of the CH_3 protons that produce equivalent fields at the CH proton determine the degeneracy. The eight permutations of the CH_3 spins shown in Fig. 2 thus lead to a predicted intensity ratio of 1:3:3:1 for the CH multiplet. Similarly, the CH_3 doublet peaks will be of equal intensity, with a total integrated intensity three times that of the CH peaks. In a more general sense, it can be seen that n equivalent protons interacting with a different proton will split its resonance into $n + 1$ lines whose relative intensities are given by coefficients of the terms in the binomial expansion of the expression $(\alpha + \beta)^n$. Equivalent protons also interact and produce splitting in the energy levels. However, these splittings are symmetric for upper and lower energy states, so no new NMR resonances are produced.

If a proton is coupled to more than one type of neighboring nucleus, the resultant multiplet pattern can often be understood as a simple stepwise coupling involving different J values. For example, the CH_2 octet that occurs for pure $\text{CH}_3\text{CH}_2\text{OH}$ (Fig. 3) arises from OH doublet splitting ($J = 4.80$ Hz) of the quartet of lines caused by coupling ($J = 7.15$ Hz) with CH_3 . It should be mentioned that such regular splitting and intensity patterns are expected for two nuclei A and B only if $|\nu_A - \nu_B| \geq 10J_{AB}$. The spectra for this weakly coupled case are termed *first-order*. Since the difference $\nu_A - \nu_B$ (in Hz) increases with the field while J_{AB} does not, NMR spectra obtained with a high-field instrument (400 MHz) are often easier to interpret than those from a low-field spectrometer (60 MHz). However, even if the multiplets are not well separated, it is still possible to deduce accurate chemical shifts and J values using slightly more involved procedures, which are outlined in most texts on NMR spectroscopy.¹⁻⁵ Such an exercise can be done

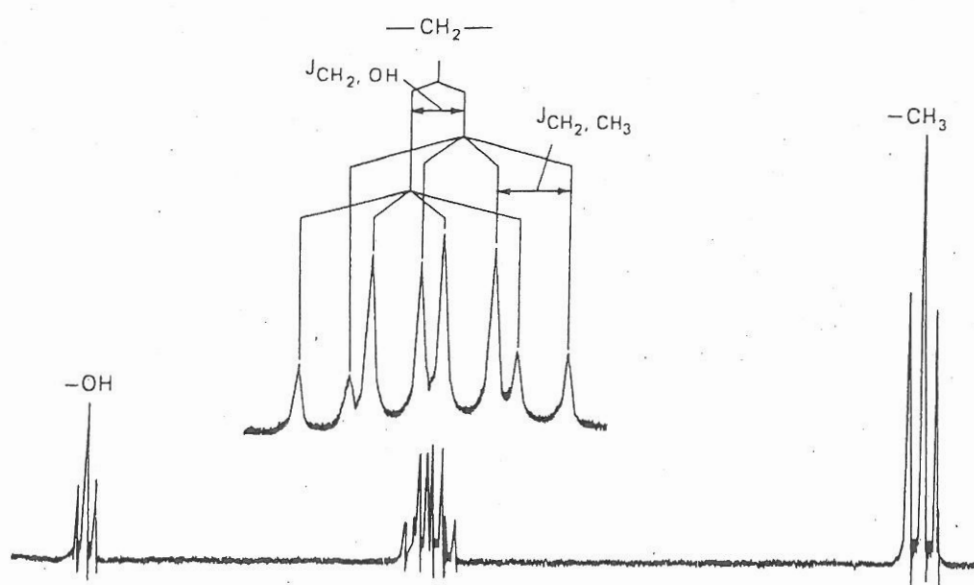


FIGURE 3

NMR spectrum of highly purified ethanol obtained at 100 MHz.

FIGURE 4

Illustration of nuclear spin-spin interaction transmitted via polarization of bonding electrons. The two electrons about each carbon will tend to be parallel, since this arrangement minimizes the electron-electron repulsion (Hund's rule for electrons in degenerate orbitals).



as an optional part of this experiment, although it will not be necessary for the determination of equilibrium constants.

The mechanism of spin-spin coupling is known to be indirect and to involve the electrons in the bonds between interacting nuclei. The spin of the first nucleus A is preferentially coupled antiparallel to the nearest bonding electron via the so-called Fermi contact interaction, which is significant only when the electron density is nonzero at the first nucleus. (Such is the case only for electrons in *s* orbitals, since *p*, *d*, and *f* orbital wavefunctions have zero values at the nucleus.) This electron-spin alignment information is transmitted by electron-electron interactions to the second nucleus B to produce a field which thus depends on the spin orientation of the first nucleus (Fig. 4). Since the strength of this interaction falls rapidly with separation, only neighboring groups produce significant splitting. A few typical spin-spin coupling constants are given in Table 2 and these along with the chemical shifts, serve to identify proton functional groups. As mentioned above, the multiplet intensities also give useful information about neighboring groups. Thus NMR spectra can provide detailed structural information about large and complex molecules.

Keto-Enol Tautomerism. It is well known that ketones such as acetone have an isomeric structure, which results from proton movement, called the enol tautomer, an unsaturated alcohol:

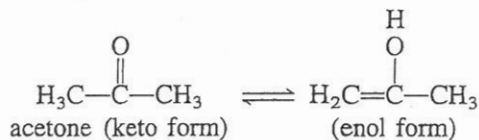
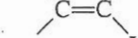
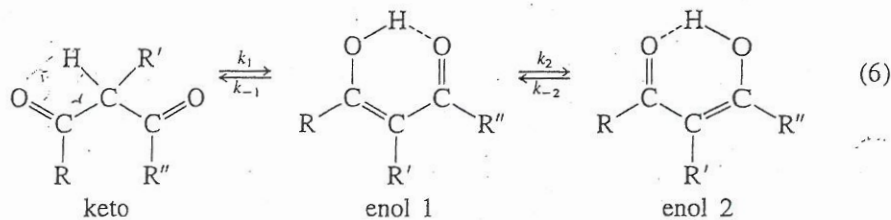


TABLE 2 Typical proton spin-spin coupling constants

COUPLING	$J(\text{Hz})$	COUPLING	$J(\text{Hz})$	
	-20 to +5		0 to 3.5	
	2 to 9		6 to 14	
	0			
	ortho- meta- para-	6 to 9 1 to 3 1		11 to 19

For acetone, and the majority of cases in which this keto-enol tautomerism is possible, the keto form is far more stable and little if any enol can be detected. However, with β -diketones and β -ketoesters, such factors as intramolecular hydrogen bonding and conjugation increase the stability of the enol form and the equilibrium can be shifted significantly to the right.



The proton chemical environments are quite different for the keto and enol tautomers, and the interconversion rate constants k_1 and k_{-1} between these forms are small enough that distinct NMR spectra are obtained for both forms. In principle, the two enols are also distinguishable when $R' \neq R''$. However, the intramolecular OH proton transfer is quite rapid at normal temperatures, so that a single (average) OH resonance is observed. In general, such averaging occurs when the conversion rates k_2 and k_{-2} (in Hz) exceed the frequency separation $\nu_1 - \nu_2$ (also in Hz) of the OH resonance for the two enol forms.² The magnetic field at the OH proton is thus averaged and resonance occurs at $(\nu_1 + \nu_2)/2$. Similarly, rapid rotation about the C—C bonds of the keto form explains why spectra due to different keto rotational conformers are not observed. Thus, distinct spectra are expected only for the two tautomers, and these can be used to determine the equilibrium constant for keto-to-enol conversion:

$$K_c = \frac{(\text{enol})}{(\text{keto})} \quad (7)$$

where parentheses denote concentrations in any convenient units.

(5)

The keto arrangement shown in Eq. (6) is the configuration which is electrostatically most favorable, but the steric repulsions between R and R'' groups will be larger for this keto form than for the enol configuration. Indeed, experimental studies have confirmed that the enol concentration is larger when R and R'' are bulky.⁴ This steric effect is less important in the β -ketoesters, in which the R ··· R'' separation is greater. For both β -ketoesters and β -diketones, α substitution of large R' groups results in steric hindrance between R' and R (or R'') groups, particularly for the enol tautomer, whose concentration is thereby reduced. Inductive effects have also been explored; in general, α substitution of electron-withdrawing groups such as —Cl or —CF₃ favor the enol form.⁴

The solvent plays an important role in determining K_c . This can occur through specific solute-solvent interactions such as hydrogen bonding or charge transfer. In addition, the solvent can reduce solute-solute interactions by dilution and thereby change the equilibrium if such interactions are different in enol-enol, enol-keto, or keto-keto dimers. Finally, the dielectric constant of the solution will depend on the solvent and one can expect the more polar tautomeric form to be favored by polar solvents. Some of these aspects are explored in this experiment.

EXPERIMENTAL

The general features of a CW NMR spectrometer were described briefly in Exp. 33, and details about Fourier-transform NMR instruments are given in Exp. 43. For the

spectrometer you are to use, more specific operating instructions will be provided by the instructor. Obtain several milliliters each of acetylacetone ($\text{CH}_3\text{OCH}_2\text{COCH}_3$, M.W. = 100.11, density = 0.98 g cm^{-3}) and ethyl acetoacetate ($\text{CH}_3\text{CH}_2\text{OCOCH}_2\text{COCH}_3$, M.W. = 130.45, density = 1.03 g cm^{-3}). Prepare small volumes of two solvents and three solutions.

Solvent A: Carbon tetrachloride, spectrochemical grade (M.W. = 153.83, density = 1.58 g cm^{-3}) with 5 percent-by-volume tetramethylsilane (TMS) added. Prepare in a 10-mL volumetric flask.

Solvent B: Methanol, spectrochemical grade (M.W. = 32.04, density = 0.791 g cm^{-3}) with 5 percent-by-volume TMS added. Prepare in a 5- or 10-mL volumetric flask.

Solution 1: 0.20 mole fraction of acetylacetone in solvent A

Solvent 2: 0.20 mole fraction of acetylacetone in solvent B

Solvent 3: 0.20 mole fraction of ethyl acetoacetate in solvent A

Use a 1-mL pipette graduated in 0.01-mL increments to measure out 0.010 mol of solute, and use a 2-mL graduated pipette to then add the correct amount (0.040 mol) of solvent. You may neglect the presence of the 5 percent TMS when determining the necessary volumes of solvent. **Warning:** All work with TMS should be carried out in a hood. All containers or samples containing TMS should be tightly sealed and stored at low temperatures because of its volatility.

Prepare an NMR tube containing about 1 in. of solvent A and another containing solvent B, and record both NMR spectra, setting the TMS signal at the chart zero. Repeat for solutions 1 to 3, taking care to scan above $\delta = 10$ ppm since the enol OH peak is shifted substantially downfield. Determine which peaks are due to solute and measure chemical shifts for all solute features. Integrate the bands carefully at least three times, expanding the vertical scale by known factors as necessary in order to obtain accurate relative intensity measurements.

CALCULATIONS

Assign all spectral features using Table 1 and other NMR reference sources.^{2,3,5} Tabulate your results and use your integrated intensities to calculate the percentage enol present in solutions 1 to 3. If possible, use the total integral corresponding to the sum of methyl (or ethyl), methylene, methyne, and enol protons. If this proves difficult because of overlap with solvent bands, indicate clearly how you used the intensities to calculate the percentage enol.

For both the enol and the keto forms, compare experimental and theoretical ratios of the integrated intensities for different types of protons (e.g., methyl to methylene protons in the keto form).

Using Eq. (7), calculate K_c and the corresponding standard free-energy difference ΔG^0 for the change in state keto \rightarrow enol in each solution.

DISCUSSION

Discuss briefly your assignments of chemical shifts and spin–spin splitting patterns of acetylacetone and ethyl acetoacetate. Which compound has a higher concentration of enol form, and what reasons can you offer to explain this result? What changes would you expect in the NMR spectra of these two compounds if the interconversion rate between enol structures were much slower?

Compare the value of K_c for acetylacetone in CCl_4 with that in CH_3OH . What does

by the
M.W. =
 COCH_3 ,
ents and

33, den-
e (TMS)
: 0.791 g
r 10-mL

0 mol of
0 mol) of
he neces-
n a hood.
d at low

ontaining
o. Repeat
I peak is
measure
ee times,
accurate

ources.^{2,3,5}
tage enol
ie sum of
ecause of
culate the
l ratios of
e protons
ifference

g patterns
tration of
ould you
between
What does

your result suggest regarding the relative polarity of the enol and keto forms? Which form is favored by hydrogen bonding and why?

Compare your values of ΔG^0 with those for the gas phase ($\Delta G^0 = -9.2 \pm 2.1 \text{ kJ mol}^{-1}$ for acetylacetone, $\Delta G^0 = -0.4 \pm 2.5 \text{ kJ mol}^{-1}$ for ethyl acetoacetate).⁶ What solvent properties might account for any differences you observe?

Additional compounds suitable for studies of steric effects on keto-enol equilibria include α -methylacetone ($\text{CH}_3\text{COCHCH}_3\text{COCH}_3$), diethylmalonate ($\text{CH}_3\text{CH}_2\text{OCOCH}_2\text{COOCH}_2\text{CH}_3$), ethyl benzoylacetate ($\text{C}_6\text{H}_5\text{COCH}_2\text{COOCH}_2\text{CH}_3$), and *t*-butyl acetoacetate ($\text{CH}_3\text{COCH}_2\text{COOt-Bu}$). Some other possible compounds are listed in Refs. 4 and 5. Further aspects of this equilibrium that could be studied include the effects of concentration, temperature, and solvent dielectric constants on K_c .⁵

SAFETY ISSUES

Carbon tetrachloride and tetramethylsilane (TMS) are both toxic chemicals; see p. 197 for details about CCl_4 . TMS is volatile and must be kept in a tightly sealed container. Carry out all solution preparations in a fume hood.

APPARATUS

NMR spectrometer with integrating capability; several 5- and 10-mL volumetric flasks; precision 1-mL and 2-mL graduated pipettes; NMR tubes; spectrochemical-grade CCl_4 and CH_3OH ; tetramethylsilane, acetylacetone, and ethyl acetoacetate; fume hood.

REFERENCES

1. J. C. Davis, Jr., *Advanced Physical Chemistry: Molecules, Structure, and Spectra*, Wiley-Interscience, New York (1965).
2. J. A. Pople, W. G. Schneider, and H. J. Bernstein, *High Resolution Nuclear Magnetic Resonance*, McGraw-Hill, New York (1959); C. P. Slichter, *Principles of Magnetic Resonance*, 2d ed., vol I in P. Fulde (ed.), *Solid State Sciences*, Springer-Verlag, Berlin/New York (1980).
3. Compilations of NMR chemical shifts and coupling constants are given in F. A. Bovey, *NMR Data Tables for Organic Compounds*, vol. I, Wiley-Interscience, New York (1967), and in L. F. Johnson and W. C. Jankowski, *C-13 NMR Spectra*, Wiley-Interscience, New York (1972).
4. J. L. Burdett and M. T. Rogers, *J. Amer. Chem. Soc.* **86**, 2105 (1964).
5. M. T. Rogers and J. L. Burdett, *Can. J. Chem.* **43**, 1516 (1965).
6. M. M. Folkendt, B. E. Weiss-Lopez, J. P. Chauvel, Jr., and N. S. True, *J. Phys. Chem.* **89**, 3347 (1985).

GENERAL READING

- R. J. Abraham, J. Fisher, and P. Lofthus, *Introduction to NMR Spectroscopy*, Wiley, New York (1991).
- R. Drago, *Physical Methods for Chemists*, 2d ed., chaps. 7, 8, Saunders, Philadelphia (1992).
- R. K. Harris, *Nuclear Magnetic Resonance Spectroscopy*, Longman, London (1986).
- C. P. Slichter, *op. cit.*

1.2.2. NMR experiments

1.2.2.1. NMR sample preparation

Delipidated fractions containing LFABP were pooled, concentrated and exchanged into the buffer (100 mM KCl, 50 mM KH₂PO₄, 5 μM EDTA, 0.02% NaN₃, pH 7.0) conventionally used for NMR experiments. The desired concentrations for acquisition of two-dimensional (HSQC) and three-dimensional (TOCSY-HSQC, NOESY-HSQC) NMR spectrum are in the range of 0.1-0.3 mM and 0.4-0.8 mM respectively. Concentration was determined using Nanodrop (Wilmington, DE) with 6400 M⁻¹ cm⁻¹ as the absorption coefficient of LFABP⁷. 5% by volume D₂O was added to 500 μl NMR sample for a ²H lock signal and it was put into a 5mm NMR tube.

1.2.2.2. 2D ¹⁵N HSQC

¹⁵N-HSQC spectra were recorded using a Varian four-channel spectrometer with ¹H frequency at 600 MHz (conventional probe). In specific cases, a Varian instrument with cryoprobe was also used. Alternatively, a Bruker four-channel spectrometer with cryoprobe was used. ¹⁵N-HSQC spectra were recorded with 1024 points in the direct dimension, 256 points in the indirect dimension and with 32 transients, unless otherwise mentioned. The data were processed with NMRpipe software²⁰, with typical parameters as shown in Table 1.1 and analyzed with NMRViewJ²¹.

nmrPipe -in test.fid	\Format Input
nmrPipe -fn SOL -fl 32	\solvent filter
nmrPipe -fn SP -off 0.35 -end 1.00 -pow 2 -c 0.5	\Window
nmrPipe -fn ZF -auto	\Zero-fill
nmrPipe -fn FT -auto	\Fourier-tranform
nmrPipe -fn PS -p0 41.00 -p1 0.00 -di -verb	\Phase, delete imaginaries

nmrPipe -fn POLY -auto -ord 0	\Auto-baseline correct
nmrPipe -fn EXT -left -sw	\Extract the left half
nmrPipe -fn TP	\Transpose X/Y
nmrPipe -fn LP -x1 1 -xn 64 -ord 10 -f -pred 64 -after	\Linear prediction
nmrPipe -fn SP -off 0.35 -end 1.00 -pow 2 -c 0.5	\Window
nmrPipe -fn ZF -auto	\Zero-fill
nmrPipe -fn FT -alt	\Fourier transform
nmrPipe -fn PS -p0 0.0 -p1 0.00 -di -verb	\Phase correct, delete imaginaries
nmrPipe -fn TP	\Transpose X/Y
nmrPipe -fn POLY -auto -ord 0	\Auto-baseline correct
-ov -out test.dat	\Format output

Table 1.1. Annotated conversion script used for HSQC spectrum recorded in Bruker 500 spectrometer at pH 7.0, 283K.

1.2.2.3. Double resonance experiments and NMR assignment of LFABP

a) Three-dimensional TOCSY-HSQC and NOESY-HSQC

TOCSY-HSQC and NOESY-HSQC data were acquired for confirming backbone resonance assignments of apo and oleate liganded holo-LFABP with 1024 complex points in t_1 , 256 complex points in t_2 and 128 complex points in t_3 . 32 transients were acquired using a four-channel Bruker 500 MHz spectrometer with a cryoprobe. Similar experiments were recorded for backbone resonance assignments of the warfarin-oleate-LFABP complex.

1.2.2.4. Titration followed by NMR

^{15}N -HSQC experiments were recorded with sequential addition of specific ligand solutions (oleate, linoleate) into apo-LFABP at 10°C. Typically, aliquots of a 2 mM stock solution of sodium oleate at pH 9.0 were added to 0.14 mM apo-LFABP in 100 mM KCl, 50 mM KH_2PO_4 , 5 μM EDTA, 0.02% NaN_3 , pH 7.0 buffer. The titration points recorded were 1:0.26, 1:0.5, 1:0.65, 1:0.78, 1:0.9, 1:1.16, 1:1.68, 1:1.95, 1:2.97 and 1:4 equivalent of protein: ligand. At the end of

the titration series, the dilution factor was 1.13 times owing to the addition of aliquots of ligand solution.

In case of linoleate, a pH 9.0, 1 mM stock solution was used and the titration points recorded were 1:0.08, 1:0.17, 1:0.25, 1:0.42, 1:0.6, 1:0.77, 1:0.94, 1:1.3, 1:1.6, 1:1.97, 1:2.5, 1:3 with similar pH and temperature as oleate. At the end of the titration series the dilution factor was 1.12 times owing to the addition of aliquots of ligand solution.

For warfarin, the titration series presented herein, started with holo-LFABP liganded with 2 equivalents of oleate. 10 mM warfarin dissolved in sodium hydroxide was used to record 0.4, 0.8, 1.2, 1.6, and 2 equivalents of added warfarin to holo-LFABP complex.

For a trial with phytanic acid, starting with apo-LFABP, 3 equivalents were added from 5mM solution of isomers of phytanic acid in NaOH and HSQC spectrum was recorded.

For glucose, excess of glucose (10 equivalents) 10 mM solution was added to apo-LFABP and HSQC spectrum was recorded.

1.2.2.5. Chemical shift perturbation analysis

Upon sequential addition of ligand solution to ^{15}N -LFABP NMR samples, the HSQC peaks of certain residues of the apo-protein spectrum may be perturbed due to a change in the chemical environment as a consequence of the interaction of the protein with the ligand. This chemical shift perturbation (in ppm) was calculated using the formula $[(\delta_{\text{Hapo}} - \delta_{\text{Hholo}})^2 + \{(\delta_{\text{Napo}} - \delta_{\text{Nholo}})/6.51\}^2]^{1/2}$, where δ_{H} is the proton chemical shift, whereas δ_{N} is the nitrogen chemical shift²².